THE STOPPING POWER OF VARIOUS SUBSTANCES FOR LOW ENERGY PROTONS

Thesis By

Michel Bader

In Partial Fulfillment of the Requirements

for the Degree of

Doctor of Philosophy

California Institute of Technology

Pasadena, California

1955

ACKNOWLEDGEMENTS

It is with pleasure that I acknowledge the assistance of Professor Ward Whaling, who supervised, from the start, all of the work described in this thesis. I am grateful to him for his many constructive criticisms and valuable suggestions. I am thankful to Professor C. C. Lauritsen, who suggested the micro-balance method, and to Professor R. F. Christy for several helpful discussions.

I am deeply indebted to Mr. R. E. Pixley, with whom nearly all phases of this work have been discussed, for his constant help throughout many long hours of operating the electrostatic accelerator. I am also very appreciative of the time he spent trouble-shooting and repairing many parts of the apparatus.

I wish to thank Mr. V. F. Ehrgott for his help on several design problems; and Messrs. G. Fastle and J. Macallister for their assistance in the machine shop.

Miss R. Niewood did all of the typing in connection with this thesis. I am deeply grateful to her for her promptness and patience with my manuscripts.

I wish to express my gratitude to the Institute for the scholarships and assistantships I have held throughout my graduate years. The experimental work was supported by the joint program of the Office of Naval Research and the Atomic Energy Commission.

ABSTRACT

The stopping cross sections of several substances were measured for protons in the energy range 50 to 600 kev. The substances investigated were lithium, beryllium, copper, gold, lead, lithium fluoride and calcium fluoride.

The energy loss in the substance under investigation was determined by measuring the incident proton beam energy necessary for a given outgoing energy before and after a thin evaporated layer of the substance had been placed in the path of the beam. The areal density of the layer was accurately determined by one of two methods: A chemical analysis or a micro-balance weighing of a known area of the evaporated deposit. The same layer was used in the energy loss as in the density determinations. These absolute measurements were made near 350 kev. Relative energy loss measurements were made over the remainder of the range, and normalized to them. The apparatus was so designed that the evaporations, weighings and energy loss determinations could be performed without removing the substance from the vacuum.

TABLE OF CONTENTS

I. INTRODUCTION

Whenever a charged particle, e.g. a proton, passes through a substance, it loses a certain fraction of its energy. The stopping cross section per atom (molecule) as a function of energy, $\epsilon(E)$, is, by definition, equal to $-(1/N)(dE/dx)$, where N is the number of atoms (molecules) per cm^3 in the stopping material and dE/dx is the energy loss of the incident particle per cm along its path. With energy in ev, ϵ will then have the units of ev-cm^2 (per atom or molecule).* Absolute measurements are actual values of $\epsilon(E)$. Relative measurements are ratios of ϵ's for the same linear thickness of substance at different energies, and are hence independent of N and dx; they depend for their usefulness on normalization to an absolute measurement at some energy.

The reasons for measuring stopping cross sections have been discussed many times by different authors in introduction to their papers, and can be found throughout the references listed in this thesis. They will be briefly reviewed here.

The stopping effect itself, which is due primarily to collisions of the incident particle with atomic electrons, is of considerable theoretical interest. Theoretical expressions for the dependence of ϵ on energy and on the properties of the interacting particles have been derived by several authors, notably H. A. Bethe[1] and N. Bohr [2]. Because of the complexity of the atomic systems, however, approximations

---

* Some authors define the stopping cross section as the energy loss per mg/cm^2 of stopping material. In these units, ϵ increases with diminishing atomic weight, while the opposite is true in our units.

have been made which restrict their applicability. These formulas gradually lose their validity as one considers lower energy ranges. Near 500 kev only fair agreement between theory and experiment is achieved, while below 200 kev, the stopping mechanism is understood qualitatively only. This lower range, between 50 and 600 kev, is the one investigated experimentally in this work.

Quite apart from their theoretical interest, stopping cross sections have had an important use in experimental nuclear physics since the very earliest days when range-energy measurements, the integral form of the $\epsilon(E)$ function, were used to determine particle energies from their ranges. More recently, the differential form dE/dx has supplanted the range-energy curve in interest in laboratories working on accurate determinations of nuclear reaction rates and energies. Briefly, the importance of dE/dx arises from the fact that an experimental measurement of a reaction rate determines the yield from a thickness of target dx containing Ndx atoms, and it is necessary to know Ndx in order to calculate the quantity of interest, the reaction rate per target nucleus. (The reason for this range dx is usually the finite resolution of the detecting apparatus.) The thickness dx is often of the order of 10^{-5} cm or less, and is consequently difficult to measure. Furthermore, it is not always certain that N, the number of atoms per cm^3 in a layer of material only a few hundred or thousand atoms thick, is the same as in the material in large quantities. Both of these difficulties can be avoided if the stopping cross section (1/N)dE/dx is known for the target being studied, since dE can be measured readily by several direct methods, or can be determined indirectly from thick target yields.

In recent years, therefore, the principal incentive for the study of stopping cross sections has come from their usefulness in interpreting nuclear reaction data.

The extensive work which has been done on proton stopping cross sections, both theoretically and experimentally, has been thoroughly summarized to June 1953 in a recent review article by Allison and Warshaw[3]. A comprehensive bibliography is included in their article. The experimental work to date on the substances of interest in this thesis will be briefly reviewed here together with some discussion of the reasons for this interest. These substances are lithium, beryllium, copper, gold, lead, lithium fluoride and calcium fluoride.

Lithium targets have been widely used in nuclear physics, and the accuracy of the computed reaction cross sections has in many cases been limited by the uncertainty in the stopping cross section of this metal for the incident particle. The energy loss of charged particle in lithium was first investigated in 1928 by Rosenblum[4] who used α-particles of 3 to 9 Mev. This was the only absolute determination of ϵ(Li) until the present work. Rosenblum used the following ingenious method to determine the linear thickness of the lithium: The target was made by compression between two accurately machined flat surfaces with a lead spacer. A jet of argon was directed on the lithium during this operation to prevent oxidation or other contamination, and the compressed lithium sheet was quickly placed in the vacuum system. The lead spacer thickness was then measured with a micrometer. An overall accuracy of 10% was claimed.

Relative measurements have been made by Haworth and King[5], and by Warters[6],[7]. These were normalized at 950 kev by Warters, who assumed the validity of Bethe's formula[1] $\epsilon(E) = (a/E) \log (bE/I)$, where a, b are constants depending on the masses and charges involved, (see sect. IV), E is the energy at which the determination is made, and I is an average ionization potential of the stopping substance independent of the incident particle. The value of I used by Warters (32 ev) was calculated by Mano[8] from Rosenblum's data. Unfortunately, the formula does not hold well at low energies, and even for α-particles from 3 to 9 Mev, a calculation of the parameter I from Rosenblum's data does not yield the same value for different energies (see sect. IV).

Like lithium, beryllium is a much investigated substance in nuclear physics, and the accuracy of the experimental results is often limited by the uncertainty in ϵ(Be). Beryllium was investigated between 30 and 500 kev by Warshaw[9]. His results do not continue very smoothly the higher energy curves obtained by Madsen[10], Kahn[11], and Madsen and Venkateswarlu[12], which show less than 5% discrepancies among themselves (fig. 13). Work now in progress by F. Mozer of this laboratory is in agreement with the above high energy data when normalized to it (only relative measurements were made by Mr. Mozer.) But those results are then 15% above Warshaw's from 200 to 400 kev, where the measurements overlap. Warshaw's normalization depended on a spectro-chemical analysis of a known area of foil. His main difficulty was to obtain a large enough area of thin Be foil for an accurate measurement.

As mentioned above, the stopping cross section of the target is related, in yield measurements, to the characteristics of the detecting

apparatus. Scattering of protons from copper has been frequently used as a means of calibrating the solid angle and energy resolution of such apparatus, and this is the primary experimental importance of an accurate knowledge of ϵ(Cu). The previous measurements on copper show considerable disagreement between different observers. Madsen's data[10] is 10% below that of the Ohio State group[13],[14], which in turn is 4% below Kahn's[11] (fig. 15). The slopes are in good agreement, and the discrepancies in normalization are attributed to non-uniformity of the foils used. Madsen used commercial rolled foils, and their thickness was determined by weighing of a large area of foil; the transmission experiments could have taken place in a part of the foil of thickness different from the average.

The experimental situation for gold is worse than for copper. Different observers[9],[10],[11],[15] report points as much as 15% apart in normalization, and with considerable spread about their individual mean curves (fig. 17). Here again, the non-uniformity of commercial foils is blamed. Work just completed by the Ohio State group[14] has made use of a weighing of evaporated deposit method akin to that described further in this work. Their results lie about 14% above an average curve drawn through the previous observers' points. The interest in gold foils stems primarily from their widespread use in slowing down charged particles.

The only data on lead at low energies comes from Ohio State[14], and Rosenblum[4] gives α-particle data from 3 to 9 Mev. Lead was investigated to obtain additional data in the region of high atomic numbers.

Calcium fluoride and lithium fluoride have not been previously investigated. Their current interest arises primarily from their use as fluorine targets. In the absence of experimental values of ϵ, interpolations have been made between neighboring elements, and molecular stopping cross sections assumed to be the sum of the atomic cross sections. This procedure is somewhat questionable, especially at low energies(this is discussed in detail in section IV).

The present work was therefore undertaken to provide additional and more accurate data below 600 kev and help resolve some of the existing discrepancies. Several refinements and improvements were introduced on the weighing method of determining areal densities. In particular, the weighing apparatus was designed a) with a greater sensitivity required because of the thinner foils used at low energies and b) so as to allow the complete operation, from first weighing through energy loss measurement to final weighing, to be performed in vacuo, without opening the target chamber. While the vacuum operation was of course essential for lithium, it was found of little importance in other cases. An additional method was used for lithium, involving a chemical determination of the deposit thickness. Both absolute and relative measurements were made.

The general principles and experimental procedure of this work will be described in part II, leaving out selected special techniques and apparatus to be treated at greater length in part III. The results will be presented in tabular form and graphically. A discussion will be given in part IV and a summary of errors in part V.

II. EXPERIMENTAL METHOD

1. Absolute Measurements

The proton beam from the 600 kev electrostatic generator passed through an electrostatic analyzer into the target chamber, where it was scattered by a gold target into a magnetic spectrometer. The particles were then detected and counted by a scintillation counter. The magnetic field was held fixed. When the number of counts in such an experiment is plotted as a function of the energy of the beam from the analyzer, a step curve results with a sharp leading edge and a flat top (fig. 1). If a foil is now placed in the way of the beam, between the target and the spectrometer, the step will appear at a higher energy. The difference between these two energies is then clearly the energy lost in the foil; and when the substance to be investigated is evaporated on the foil, the additional energy required of the scattered beam, in order to go through the foil and be accepted by the spectrometer, is the energy loss in the substance. A typical set of such step curves is shown in fig. 1. It is worthwhile to note that, with this method, the exact thickness of the supporting foils need not be known. These supporting foils had to be used because of the difficulty of obtaining thin enough uniform self-supporting foils of the substances of interest.

These energy losses as measured by analyzer settings must of course be corrected by a constant multiplying factor which takes into account the difference in energy between the incident and scattered beam. A simple calculation based on the momentum and energy conservation laws

yields:

$$\frac{E_2}{E_1} = \left[\frac{M_1}{M} \cos\theta \pm \left(\frac{M_o - M_1}{M} + \frac{M_1^2}{M^2} \cos^2\theta \right)^{1/2} \right]^2 \qquad \text{(II-1)}$$

where E_2/E_1 is the ratio of scattered to incident energy, M_o is the mass of the target nucleus (assumed at rest initially), M_1 is the mass of the incident particle, $M = M_o + M_1$, and θ is the scattering angle in the laboratory. E_2/E_1 is evidently a fixed quantity throughout a measurement, since only the energy E_1 is varied.

With this technique as a base, three somewhat different experiments were performed, depending on the method used to measure the areal density of the substance under investigation.

a) Lithium: An aluminum foil (see fig. 2) was placed immediately behind a 0.250" hole in the center of a 5 mil tantalum sheet of about 2 by 4 inches. The exposed area of tantalum was defined by a carefully assembled square steel frame of accurately known dimensions. This assembly was mounted on a system of lever arms which allowed a lateral motion of about two inches; the tantalum sheet was put in a vertical plane near the entrance to the spectrometer. The lithium furnace was diametrically opposite in the target chamber. The target was of 1/2" round brass stock, with two flats milled 180° apart; it could be raised out of the way and rotated through an O-ring seal without disturbing the vacuum. A thick evaporated gold layer was present on the inner flat, as shown in the figure, where the target is in the "out of the way" or "evaporating"

position. A removable shield, placed immediately in front of the furnace, permitted lengthy preliminary out-gassing. Pressures during evaporation were held below 10^{-4} mm of Hg.

The experiment then proceeded as follows. The position of the gold step was first measured with the foil in the way of the scattered beam. The target was raised, lithium was evaporated and the new position of the gold step was determined with the target back in scattering position (fig. 1).

Before re-opening the target chamber, the following experiment was performed to determine the amount of impurities, if any, in the evaporated lithium. The entire tantalum and aluminum foil assembly was swung out of the way, and the outer flat of the target, now covered with lithium, was exposed to the beam. In accordance with eq. II-1, with E_2 fixed by the setting of the spectrometer and θ kept constant (here 90°), the energy E_1 at which particles are counted depends on the mass of the scattering nucleus. Thus a plot of the number of counts versus E_1 is expected to show what nuclei are present in the target.* A negligible surface contamination of oxygen was found in this way (fig. 3), as well as a negligible amount of carbon, which increased with bombardment time and was probably altogether absent on the foil. As can be estimated from the figure, the aggregate thickness of contaminants was under 0.25 kev, while the lithium layer was 100 kev thick.

---

* This technique of surface analysis was first described by Snyder, et al. (17).

Argon was let into the target chamber instead of air, and the tantalum collector was placed in a clean beaker with distilled water, care being taken not to lose any lithium or contaminate the collector by handling. The argon was used as a precaution to prevent a loss of lithium from the collector during the sudden heating which occurs when the exposure to air and resulting lithium oxidation are less gradual. The hydroxide was titrated (see sect. V) against a standard solution of HCl (obtained from the Braun Corporation, Los Angeles; they claim 0.2% accuracy in their standardization). Thus, the total amount of lithium on the collector was determined.

In order to determine the density of the lithium at the center, where the transmission experiment took place, it was assumed that the evaporation took place in straight lines from a small source (the 1/8" exit hole of the furnace; see section III, part 4). The furnace exit hole was carefully aligned horizontally with the aluminum foil (fig.2), and the distance between them accurately measured with an inside micrometer; this distance was made as large as possible to minimize the amount of variation of the density across the collector. The further assumption was made that the evaporation process could be treated as the effusion of a gas through a small hole into a vacuum.

On the basis of these assumptions (see checks below), the geometrical corrections are calculated as follows. The amount of deposit dI on a small area dxdy of the collector will be proportional to dxdy and to the furnace exit hole area, both projected on a plane perpendicular to the direction of the lithium beam to that point; and inversely proportional to the square of the distance r between dxdy and the furnace

exit hole. We have therefore

$$dI = k \frac{dx\, dy}{r^2} \cos^2 \Psi = k \frac{R^2\, dx\, dy}{(R^2 + x^2 + y^2)^2} \qquad \text{(II-2)}$$

where R (see fig. 4) is the perpendicular distance from the furnace to the collector, Ψ is the angle between R and r, and k is a proportionality constant. If the dimensions of the collector are 2a by 2b, and the source is aligned with the center of the collector, the total deposit will be given by

$$I = 4kR^2 \int_0^a \int_0^b \frac{dx\, dy}{(R^2 + x^2 + y^2)^2} \qquad \text{(II-3)}$$

$$= 2k \left[\frac{a}{\sqrt{R^2 + a^2}} \tan^{-1} \frac{b}{\sqrt{R^2 + a^2}} + \frac{b}{\sqrt{R^2 + b^2}} \tan^{-1} \frac{a}{\sqrt{R^2 + b^2}} \right]$$

From this we must subtract the amount which went through the center hole, of area A, in the collector. With A small and R large, $\cos \Psi \approx 1$ and $r \approx R$ so that this amount will be quite accurately given by kA/R^2. Since the aluminum foil was a small distance s behind the collector, the area B over which the lithium was spread is given by $A(R+s)^2/R^2$. We have then as a final formula for the area density of deposit on the foil

$$\rho = \frac{kA/R^2}{B\,(I - kA/R^2)}\, D \qquad \text{(II-4)}$$

where D is the actual amount of deposit on the collector as measured by the titration. It is seen from the equation for I (II-3) that the constant k cancels out of the equation for ρ (II-4). Since the geometry was not exactly reproducible from one experiment to the next, the quite cumbersome computation of the parameters in eq. II-4 was repeated each time.

In order to check the validity of eq. II-3, several evaporations were made in an evacuated bell jar, with approximately the same geometry as in the target chamber. The collecting foil was however split into three strips, so that each one could be chemically analyzed separately. Evaporations were made with the strips lined up vertically and also horizontally. The ratios of the amount of deposit on each of the side strips A and B to that on the center strip C were measured for various furnace to foil distances and compared with the predictions of eq. II-3. The results are shown in figure 5, from which we see that there is a discrepancy of about 2% at R = 5 inches. The error involved was actually not that large because the total exposed area was larger in the bell jar than in the target chamber. A correction amounting to 1.5% was therefore adopted and applied to the final results on the basis of these experimental checks.

The assumption of line of sight evaporation was borne out by the sharp shadows of objects in the target chamber; for the same reason, it was not thought that the lithium atoms rebounded from several surfaces before settling down. The gaseous effusion type of evaporation from the furnace assumes that the mean free path of the particles is large compared to the diameter of the exit hole. An order of magnitude calculation gave a mean free path of 10^2 to 10^3 cm, while the hole diameter

was 0.32 cm. The above 2% discrepancy was finally explained by the observation that if the edges of the exit hole had a finite thickness, the evaporation would be greater in the forward direction, which is precisely what was observed. An analytical computation of this effect was algebraically prohibitive because of the geometry involved, but an order of magnitude estimate based on a square exit hole gave a correction in agreement with that found experimentally.

The stopping cross-section of lithium was also measured by the micro-weighing method described in part c) below.

b) Beryllium: An evaporated beryllium foil of approximate areal density 0.2 mg/cm^2 * was mounted on a movable holder so designed (see section III, part 3) that the foil could be reproducibly placed in different positions with respect to the scattered proton beam. To determine the energy loss in this foil, the position of the gold step was alternately measured with the foil in and out of the scattered beam. This operation was repeated for a series of spectrometer settings, thus yielding energy losses at different mean energies. The energy thickness was also measured at five different spots on the foil by changing the foil holder position. Less than 1% variation was found in four cases; the fifth measurement was discovered to have been located on a visibly damaged portion of the foil. The beryllium was then placed in the target position, and scattering was observed from both sides of it to determine the amount of impurity present. Surface contaminations of oxygen, carbon and a heavier element were found (fig. 6), with an aggregate energy thickness of at most 3% of

---

* We are indebted to Professor Bradner, of the University of California, who supplied us with several such foils.

the total energy loss in the foil. The amount of this heavier element, as can be seen from the figure, was too small to determine its nature. Its atomic weight was 25 ± 5. The thickness of the impurities was determined from the half-width of the peaks in figure 6. This is clearly an over-estimate, since it can be seen from the heights of these peaks that their width was really less than the resolution of the spectrometer. As we shall see later, a closer analysis was not necessary.

An accurately known area of the foil was obtained by putting it on a flat piece of glass and brushing the beryllium away around a 3/4 inch diameter brass rod held gently but firmly on top of it. The beryllium disk so obtained did not stick to the end of the rod, but was broken into several pieces. These pieces were weighed on the micro-balance described in section III, part 1. It is estimated that less than 0.5% of the foil was lost and not weighed because of its being broken up into fine beryllium dust.

The correction for contamination can be calculated as follows. By definition,

$$\epsilon = -\frac{1}{N}\frac{dE}{dx} = \frac{A \cos\theta}{N_o}\frac{M}{W}\Delta E \qquad \text{(II-5)}$$

where ϵ has been expressed in terms of the quantities actually measured in the laboratory: A is the area of the foil; W is its weight; M is its atomic weight; θ is the angle between the proton beam and the perpendicular to the foil; ΔE is the energy loss; and N_o is Avogadro's number. We may now take the contaminant to be exclusively oxygen. This is approximately true, and furthermore oxygen makes a good average, for

our purposes, between carbon and the heavier contaminant. We then have

$$\epsilon(\text{uncorrected}) = \frac{A \cos\theta}{N_o} M(\text{Be}) \frac{\Delta E(\text{Be}) + \Delta E(0)}{W(\text{Be}) + W(0)}$$

$$= \frac{A \cos\theta}{N_o} \frac{M(\text{Be})\,\Delta E(\text{Be})}{W(\text{Be})} \frac{1 + \Delta E(0)/\Delta E(\text{Be})}{1 + W(0)/W(\text{Be})}$$

$$\epsilon(\text{uncorrected}) = \epsilon(\text{Be}) \frac{1 + \Delta E(0)/\Delta E(\text{Be})}{1 + \frac{\Delta E(0)}{\Delta E(\text{Be})} \frac{M(0)}{M(\text{Be})} \frac{\epsilon(\text{Be})}{\epsilon(0)}} \qquad \text{(II-6)}$$

In the denominator of the above equation, we take, at 350 kev, $\epsilon(\text{Be}) = 6.50 \times 10^{-15}(\pm 5\%)$ ev-cm^2 (uncorrected value); $\epsilon(0) = 11.0 \times 10^{-15}(\pm 3\%)$ ev-cm^2 (from reference 24); and $\Delta E(0)/\Delta E(\text{Be}) = 0.03$ (experimental.) With these figures, one gets $\epsilon(\text{uncorrected}) = (1.000 \pm 0.003)\,\epsilon(\text{Be})$. No correction was therefore indicated.

c) Cu, Au, Pb, Li, LiF, CaF_2: These substances were investigated by a third technique, whose description follows. A quartz fiber microbalance, installed in the vacuum system, was first calibrated and an aluminum foil was weighed according to the procedure described in section III. The gold step position was measured first without foil, then with the foil hooked in position behind a shield with a defining hole(sect. III, and fig. 7). The gold target was lowered into a brass tube serving as a shield to keep the scattering surface clean, much as in figure 2, and the substance to be investigated was evaporated onto the foil. A system of shields protected all parts of the apparatus connected with the weighing within the target chamber. The displaced position of the gold step was observed, then the foil moved out of the scattered beam and the gold step location again determined. The foil was weighed anew

to determine the amount of deposit, and the balance was recalibrated.

The positions of the gold step without foil before and after the transmission experiment showed a variation which never exceeded 2% of the energy loss in the foil. This was taken into account in the following way in the calculation of ΔE: Suppose that, in a given instance, the clean gold step had moved 2δ kev higher; then the position of the step through the clean foil, taken at nearly the same time as the first gold step, was corrected by an amount $+\delta$; and the position of the step through the foil and deposit, taken at the time of the second gold step, was corrected by $-\delta$; a probable error of δ was then assigned to ΔE. Most of the shifting was disposed of in the later days of the experiment by a) overhauling the analyzer, whose plates were heavily covered with an insulating layer of pump oil, and b) using a more sensitive galvanometer to detect spectrometer setting fluctuations.

The area of the deposit was defined by the accurately punched hole in the foil holder (sect. III, and fig. 7). A correction was applied because of the gap between the foil and the shield; this was minimized by keeping the gap small and the distance to the furnace as large as feasible. The correction then amounted to 2% or less of the area, and was itself known to better than 20%. In the cases of copper and gold, a more accurate determination was made by measuring the diameter of the deposit by means of a traveling microscope. No difference was found between this and the geometrical estimate. LiF and CaF_2 layers were not visible on top of the aluminum foil as background, so that the microscope method could not be used; neither could it be used for lithium, as the foils did not withstand the oxidation of the lithium upon contact

with air. Lead was evaporated outside the target chamber, for reasons explained in section III, part 4, and the foil was kept immediately behind the defining hole.

Liquid nitrogen cold traps were used as part of the pumping system, to condense oil vapors from the diffusion pumps as well as residual gases in the target chamber. On many occasions these cold traps had to be warmed up and the target chamber opened in the course of an experiment. The substances Cu, Au, Pb and CaF_2 exhibited no change of weight or energy thickness in the course of such an operation. Considerable confidence was picked up from these incidental measurements, and in the later days of the experiment the weighings were done in air rather than vacuum in order to save time. No disagreements with previous determinations were observed.

In all three methods discussed above, the energy to which the measurements pertained was taken as the average of the incident and outgoing energies in the substance as measured by the gold step positions. The validity of this assignment has been discussed in many of the references listed, in particular in some detail in Allison and Warshaw's review article[3]. They show that

$$E(\text{actual}) = E(\text{average}) \left(1 + \frac{1}{48} \frac{(\Delta E)^2}{E^2}\right) \qquad \text{(II-7)}$$

provided ϵ is proportional to $E^{-1/2}$, which is a good approximation near 350 kev, where these absolute measurements were made. Since the energy losses were at most half of the total energy, and usually a third to a fifth, no corrections were made.

At least two and usually three or four determinations of absolute ϵ's were made for each substance. The results are listed in table I.

2. Relative Measurements

Three different techniques were used to make relative measurements, their individual applicability depending on the atomic weight of the substance under investigation and on its availability in sufficiently thin self-supporting foils: a) gold step positions with a self-supporting foil in and out of the scattered beam; b) gold step positions as seen with an aluminum foil in the beam, and then with that same foil and a thin evaporated layer of the substance desired; and c) gold steps as seen through a thin deposit made right on the gold target. Two steps are of course taken at each spectrometer setting; one with and one without the layer of investigated substance.

a) Beryllium and Gold: Since the energy loss in the beryllium foil used for the absolute measurement was determined for various spectrometer settings, a series of absolute values were obtained. It must be pointed out, however, that they all depended on a single density determination. It might be better therefore to consider that only one absolute value was obtained (and this can be taken at any of the points) and that the remaining points are relative measurements normalized to the chosen one. Because of the thickness of the available foils, this was only carried down to 180 kev (in the range 50 to 250 kev, values were obtained as described in part c below).

The same method was used for gold, except that the foil was not

used for normalization, and that it was thin enough to go down to 50 kev.

The preparation of thin metallic foils by evaporation on plate glass and subsequent floating on distilled water has been described by Warshaw[18]. While this method is adequate for work above about 200 kev, attempts to obtain thin enough foils for work at lower energies were unsuccessful for Au, Pb and Cu (see sect. III, part 2). This is why a commercial hammered foil of gold was used. Since the same spot was used for all transmission, and the foil was not used for normalization, it was felt that reliable values were obtained.

b) Copper and Lead: Relative values for copper and lead were obtained by first measuring the energy loss of the beam in an aluminum foil at a series of spectrometer field settings. This was repeated for these same settings after a layer of substance was deposited on the foil. This method introduced an additional uncertainty, that of the reproducibility of the spectrometer settings over long periods of time. A drift was observed which amounted to as much as 3% of the energy loss in the substance over a period of about eight hours, the time required for such an experiment. A correction was made in the manner described above (part 1(c) of this section).

c) Li, Be, LiF and CaF_2: For these remaining substances, containing only elements of atomic weight much lower than that of gold, a more accurate procedure could be followed. A thin layer of the substance was evaporated directly on the gold target, and the resulting displacement of the step was measured for a series of spectrometer settings and the same spot on the deposit. An additional clean gold target was available, and the two were alternately used at each setting so that

no long periods of time elapsed between related measurements, thus making negligible the drifting mentioned in the previous paragraph. The linear thickness constancy of the layer of deposit was monitored by returning to a previous setting. In a few cases where an increase in thickness, attributed to deposited pump oil, was observed, a new spot on the target was used. Measurements were then continued, making sure that an extra one or two were taken which overlapped the previous set, so that the new spot did not have to be assumed of the same thickness as the discarded one.

What makes this method work is that the scattering from a light nucleus requires a much larger incident energy for acceptance into the spectrometer than does scattering from gold (see eq. II-1); this means that, with thin enough deposits, counts from the deposit layer did not appear until after the flat gold top was reached. Furthermore, in accordance with the well known Rutherford law, the scattering cross section is lowered by the square of the ratio of the atomic number of the light nucleus to that of gold. Hence these additional counts, even in the worst case, when calcium was on the target, amounted only to $(20/79)^2 = 0.064$ of the counts from gold (other factors entering in the total yield approximately cancel out). This means that, for all but CaF_2, the thickness of deposit was not critical as far as the resolution of the gold step was concerned. Copper presented a special problem in that a layer thin enough for the above precedure was too thin to measure accurately. A typical curve obtained with a layer of copper of about 8 kev on a gold target is illustrated in figure 8. It is easily seen from this figure that the counting rate from the copper (which starts near 92 kev) is superposed on that from the gold (which starts near 99 kev),

so that the mid-point of the gold step cannot be accurately determined. Hence the method was not applicable to copper.

The energy of the measurement, in this last method, cannot be taken as a simple average, as in the foil transmission experiments. The formula to be used here has been derived in some detail by Wenzel[19] who gives:

$$E = \frac{dE_2}{dE_1} \frac{Ea\left(1 + \frac{\cos\theta_2}{\cos\theta_1}\right) - \frac{\Delta Ea}{2}\left[1 + \frac{\left(1 + \frac{\cos\theta_2}{\cos\theta_1}\right)\frac{\cos\theta_2}{\cos\theta_1}\frac{dE_2}{dE_1}}{1 + \frac{\cos\theta_2}{\cos\theta_1}\frac{dE_2}{dE_1}}\right]}{1 + \frac{\cos\theta_2}{\cos\theta_1}\frac{dE_2}{dE_1}} \qquad \text{(II-8)}$$

where $\frac{dE_2}{dE_1}$ is obtained from eq. II-1;

Ea is the incident energy for acceptance of the scattered beam by the spectrometer at a given field setting;

$\Delta Ea = Ea - Eao$, Eao being the incident energy on clean gold for the same spectrometer setting;

θ_1, θ_2 are the angles at which the beam is incident and scattered, respectively, from the target, and are measured from the outward normal to the target.

The assumption made in deriving eq. II-8 is that the stopping cross section varies linearly with energy over the range Eao to Ea. The thicknesses of the deposits used for these relative measurements

were kept near 10 kev. This procedure justified the use of eq. II-8, and eliminated the need for a more accurate a priori knowledge of the energy dependence of ϵ.

In this experiment the scattering angle was set at 165°, the maximum obtainable with the apparatus, in order to increase the energy separation of the protons scattered from different nuclei (eq. II-1). The target was perpendicular to the incident beam, so that $\theta_1 = 0°$ and $\theta_2 = 15°$. From formula II-8, we get for this case, with protons incident on gold,

$$\begin{aligned} E &= (.98984)\ Ea - (.49244)\ \Delta Ea \\ &= (.49740)\ Ea + (.49244)\ Eao \end{aligned} \qquad \text{(II-8a)}$$

which is seen to be lower than 1/2 (Ea + Eao) by about 1%.

III. SPECIAL APPARATUS AND TECHNIQUES

1. The Micro-Balance And Its Calibration

A fairly uniform quartz fiber, 4" in length and 0.002" in diameter, was obtained by heating a quartz rod over an oxy-acetylene flame and pulling quickly with the heat removed. One end of the fiber was then bent back, thus forming a hook. The other end was firmly held between two lead washers screwed against the flat head of a 1/4-28 bolt. Lead was used because a harder material, such as brass or steel, was found to break the fiber when pressure was applied. The reproducibility of the results obtained (see below) indicated that lead was not too soft to hold the fiber firmly in place when a weight was placed on the hooked end. The fiber was aluminized (by evaporation in vacuo of aluminum onto it) in order to render it readily visible (the original purpose was to make it electrically conducting, but this was eventually not needed; see the discussion of the foil holder below).

A 3/8" steel shaft entered the target chamber horizontally through an O-ring, about one inch above and parallel to the incoming proton beam (fig. 7). Collars were set so that the shaft could rotate but not move in and out. On the outside end, a dial with a vernier was attached so that the angular displacement of the shaft from an arbitrary zero could be read to plus or minus one minute. The bolt holding the quartz fiber was then screwed to the end of the shaft inside the vacuum chamber. The dimensions were so adjusted that the fiber, when horizontal, extended from the center of the target chamber to within 1/2 to 3/4 of an inch of the wall (the inside radius of the chamber was 3-5/8").

A 45° mirror was mounted near the hook of the fiber, so that, when viewed vertically through the lucite top of the target chamber, the vertical motions of the hook appeared horizontal. This was actually viewed through a telescope fixed in position outside the chamber. When a bright light (100 watts) was shone on the fiber at a proper angle, the hook could be easily seen through the telescope; the visibility was better with a bright background which was obtained by using a copper lining on the walls of the chamber.

A weighing operation then consisted in hooking the unknown mass on the fiber and bringing the image of the end of the hook in coincidence with a fixed cross-hair in the telescope by rotating the shaft. Extreme care, of course, had to be exercised in all handling of the fiber (an ample supply of spare ones is recommended.)

The standard weights were made of 2.5 mil Kovar wire. A 20" length was accurately measured and weighed to ± 0.05 mg on an analytical balance. It was then cut under a magnifying glass into smaller lengths known to ± 0.02". The density of the wire was 0.6235 mg/inch, and weights were for convenience measured in inches of wire. The quartz fiber was calibrated every quarter of an inch, and a linear interpolation made between the points. The validity of this procedure is borne out by the high degree of linearity of the calibration curves, one of which is reproduced in figure 9. Several sets of standard weights were prepared and checked against each other; they were also checked by addition, i.e., weighing a 5" length and then a 2 and a 3" length together. The readings were reproducible to within one minute, which was the limit of accuracy of the dial. With a sensitivity of, typically, 385 min/mg (2.60 μg/min),

this meant an accuracy of 0.2% for a 3" weight, which was the smallest length used. The standards were frequently washed in acetone and handled with brass tweezers only.

In an actual experiment, a measurement was first made with a foil on the hook. Then three or four calibration points were taken, covering the range in which the foil lay. Then the foil was weighed again to check that nothing had changed. Each measurement actually consisted of an average of three or four re-settings of the hook image in coincidence with the cross-hair; the spread in these individual settings was usually 2, sometimes 3 minutes.

A constant shift in the calibration was observed when the target chamber was evacuated. This shift was reproducible, the original readings being restored when air was let in. Neither an optical nor a buoyancy effect could account for it - these were both negligible. The shift was however quite constant, so that it did not affect weight differences. It was not until after all data had been taken that the source of the trouble was discovered. It lay in a mechanical springing apart of the two halves of the target chamber. The accuracy of the procedure was not affected, in view of the constancy and reproducibility of the effect. The way to get rid of it would have been to mount all parts of the micro-balance on the top half of the target chamber (which would have been feasible, though cumbersome). The fiber was recalibrated at the time of each separate weighing. A shift in calibration was found in a few cases where the fiber had been subjected to severe heating under load.

2. The Aluminum Foils

The requirements on the aluminum foils were: a) an area of at least 1 cm^2, in order for a thin deposit to have sufficient weight to be measured accurately; b) a weight not exceeding a few milligrams, as the deposit itself was to weigh 1/2 to 1 mg; and c) an energy thickness not exceeding about 10 kev at 350 kev, in order to minimize straggling and loss of particles. In addition, the foils had to withstand 1) a fair amount of handling in the weighing process and in the process of hooking behind the holder (see part 3 below); and 2) a large amount of heating during the evaporation of the substances investigated. Foils satisfactorily meeting these requirements were made as follows.

Aluminum rings of inner and outer diameters 0.440" and 0.625" were punched out of 1/4 mil commercial foil. A special punch was designed and machined to 0.001" tolerances. These rings served as frames to hold the thin aluminum foils. Four 1/2" holes were drilled in each of several brass plates 1/8" thick. The rings were approximately centered on the holes, and held in place by a minute drop of Duco cement near one edge of the plate. This was then immersed in a pan filled with water, leading with the edge on which the cement drops were. This procedure prevented the rings from floating up to the surface and kept them centered on the holes, while at the same time little enough cement was used so that they could be later cut loose without too much difficulty.

A mixture of Duco cement and amyl acetate was prepared. When a drop of this was allowed to fall on the water, it formed a thin film which could be further spread with a wooden stick to an area 6 by 6" approximately. The thickness depended on the proportions of cement and acetate

used and was not very critical. The film was lifted out of the water by the brass plate with the rings, care being taken 1) to trim the film around the plate before removing from the water else it would curl and fold over once out of the water and 2) to lead edgewise and slowly out of the water, else the surface tension would break the film.

When dry, the plate was put in a bell jar with the ring and film side about five inches above a tungsten filament. The bell jar was slowly evacuated, and shavings of 2-S aluminum were evaporated from the filament. The evaporation was stopped as soon as the glowing filament (around 700°C) was no longer visible through the foils. In order to dissolve the cement film, the back side was covered with a few drops of acetone with the foils still on the brass plate. The foils were cut loose from the plate by gently prying around the edges with a razor blade. Once loose, they were held by one edge with brass tongs and dipped for 10 to 15 seconds in acetone to remove any residual film of cement.

Only 15 to 20% of the foils came through these operations undamaged. The survivors were however surprisingly sturdy. They were stored in a box and could lie on top of one another without being hurt, and they seldom broke during the subsequent handling (great care being taken, of course, to touch only the ring and not the center foil, and to keep away from strong drafts).

A quartz hook was made as for the micro-balance, but only about 1-1/4" long and of somewhat smaller diameter to reduce weight. This was cemented to each foil with a minute drop of Duco to provide a means for hooking on to the balance fiber. A 1" length of quartz fiber was

cemented diametrically opposite and perpendicularly to the hook; its purpose will be explained in the next section.

Complete with hook and cross-bar, the foils weighed around 3.5" (2.2 mg). Their energy thickness was 10 to 12 kev at 300 kev. They were checked for weight constancy under severe heating by exposing them to a hot tungsten filament for up to three hours. They were also checked after overnight stays in the vacuum system. No changes in weight were ever observed.

Attempts to make foils of copper and gold by the method just described for aluminum proved unsuccessful. While the aluminum foils were somewhat wrinkled before the removal of the cement film, Cu and Au evaporated deposits seemed to stretch the film and put it under great tension. This made the handling of these foils very difficult, and no adequate way was found to remove the cement film.

3. The Foil Holder

During the transmission experiment and the evaporation process, the foil was held quite stationary in back of a shield with an aperture defining the exposed area. This was done with the foil remaining hooked on the balance fiber, and in such a way that the whole assembly could be moved in and out of the way of the beam and the foil released at will for weighing, without disturbing the vacuum in the system.

A thin copper plate (1-1/2" x 2-3/4" x 1/32") with an accurately punched hole (0.4375" dia.) served as the shield. It was mounted vertically on a horizontal lever arm extending about six inches diagonally across the bottom of the target chamber (fig. 7). This arm ended in

the rack part of a pinion-and-rack arrangement, the pinion being actuated from outside through an O-ring seal. The shaft for the pinion came through a plug in the bottom of the target chamber; this plug made an O-ring seal with the chamber and could be easily rotated. The shield, then, could be moved at will along the direction of the lever arm, and along an arc perpendicular to it.

Two small wire hooks were mounted, one on each side and at the bottom of the defining hole (fig. 7). With some juggling along the several degrees of freedom available, and a fair amount of patience, the cross bar at the bottom of the foil could be slipped under these wire hooks, with the foil hanging from the balance fiber through which some tension was then applied.

Another method of holding the foil was attempted but was never entirely satisfactory. It contains several points of sufficient interest, however, to warrant a brief discussion here. The idea was to hold the foil against the shield by electrostatic attraction. All fibers were aluminized, and the cemented spot between the foil and its hook was painted over with a minute amount of aquadag. A lucite bolt on the balance shaft and a lucite plug for the pinion provided the necessary insulation. Several insulators were tried on the shield, a thin coating of glyptal clear varnish being found best. Adequate attraction was obtained with a 300 volt battery, but repulsion was very unpredictable. At one time, up to 900 volts failed to do the job, at which point sparking occurred between the shield system and the balance fiber. Another difficulty was that the thin part of the foil (as apposed to the ring) stuck very tightly to any material on which it had been pressed, and often the ring came loose but the foil was torn.

4. Evaporation Techniques

The furnaces or filaments had to be sufficiently removed from the foils so that the deposits could be assumed uniform over 1 cm^2, and so that the foils did not get over-heated. Altogether, the requirement for this experiment was a line of sight evaporation in the horizontal direction of about one gram of substance. While evaporation techniques have been previously investigated[20],[21] for many substances, our special requirements necessitated many modifications and innovations.

a) Lithium: In small amounts, this metal can be evaporated from a cubical 3 mil tantalum box with a small hole in one wall. The box is heated by conduction of current. Larger amounts of lithium short out the furnace, so that an impractical amount of current is required. In this experiment the furnace used was a cylindrical box of stainless steel, of diameter 3/4", height 7/8", and wall thickness 3/64". Near the 1/8" exit hole in its side, the wall was 1/64" thick. There was a tightly fitting lid. A 3 or 5 mil tantalum sheet was wrapped around this box; the tube thus formed by the tantalum extended one to two inches beyond the furnace at each end. The ends of this tubing were clamped to copper electrodes. The heating was then accomplished by passing current through the system. The success of this method was attributed in part to the large heating effect in the empty ends of the tantalum tubing which prevented the heat from being carried away by conduction from the furnace; and in part to the fact that molten lithium does not wet steel as readily as it wets tantalum, and hence does not run up the walls and short out the furnace. A large amount of current was still required, though the melting point of lithium is only 186°C, and the entire target chamber had to be air

cooled. The evaporation time was of the order of an hour, for 1 mg/cm^2 of deposit at a distance of 5 inches. It was found necessary to out-gas the lithium by keeping it just under its melting point for 30 minutes to an hour in the vacuum system. A removable shield was placed immediately in front of the furnace exit hole to prevent accidental evaporation onto other objects in the target chamber during the out-gassing procedure. After this treatment, lithium could be evaporated at residual gas pressures of less than 10^{-4} mm of Hg.

b) LiF and CaF_2: Both these substances, being non-conducting, are easily evaporated from cubical tantalum boxes heated by passage of electric current. The high melting point of CaF_2, 1360°C, made it necessary to air cool the chamber.

c) Gold: This metal is evaporated from a tungsten filament without too much difficulty. A very low rate had to be maintained, however, because at too high a filament temperature spattering occurs, particles occasionally being shot clear across the chamber and breaking the foil. The gold was therefore kept just above melting (1062°C) and evaporation times up to an hour and a half were not uncommon. The filaments had to be"wetted" first with a small amount of gold; if a large amount was placed on a new filament, it formed a heavy drop which fell off.

d) Copper: The high conductivity of this metal makes it unsuitable for unlined furnaces. While furnaces with Al_2O_3 linings have been described (20),(21), it was found impractical to modify them for evaporation in a horizontal direction. Several materials for filaments were investigated: tungsten, tantalum, zirconium, stainless steel, and pure copper wire. The best results were obtained with a straight length of 40 mil tantalum

wire. Small copper strips (1/16 x 5/16 x 1/32") were cut from a pure copper sheet and crimped on the filament. They were separated by about 1/2". Two were used, and the second melted only after all of the first was evaporated. There was no tendency to run all over the filament, though the wetting was sufficient to prevent falling off. Evaporation time was comparable to that for gold, and for the same reasons. It was found by scattering that no tantalum was evaporated along with the copper.

e) Lead: This metal melts at 327°C and apparently does not wet tantalum, so that the cubical tantalum box method is applicable in spite of the shorting out effect. A serious difficulty was encountered however. Lead atoms do not always stick to the surfaces which they hit, but may rebound many times before settling down. As a result, the back of the foil, well shielded as it was, was found to have about 10% as much lead as the front. The mirror and balance fiber also got coated in spite of shielding. Since it was found that the weight and thickness of lead did not change measurably on exposure to air, the evaporation was not carried out in the target chamber, but in a bell jar, with the foil enclosed in a brass box with a defining aperture. Ten seconds to a few minutes were required, depending on the amount of heating. The proper amount of deposit was estimated visually from the coating of the bell jar (since shielding was of no use).

IV. RESULTS

The numerical results are presented in tables I and II and graphically through figures 10 to 22. They will be examined here for each substance in turn.

Lithium (figs. 10, 11): Absolute values of ϵ in lithium were obtained by the chemical method at four energies, and by the weighing method at two more. These were all between 380 and 450 kev. By proper normalization, the curve through the relative values could be made to pass within $\pm$ 0.9% of five of the six points, one of the chemical points lying less than 2% lower (fig. 10).

An estimate of the stopping cross section ϵ_p (E_p) for protons of energy E_p can be made from $\epsilon_\alpha(E_\alpha)$ for α-particles by use of Bethe's formula(1)

$$\epsilon(E) = \frac{4\pi e^4}{m} \frac{z^2}{v^2} Z \ln \frac{2mv^2}{I} \qquad \text{(IV-1)}$$

where e and m are the electronic charge and mass, z and Z are the atomic numbers of the incident and target nuclei, v is the velocity of the incident particle, and I is an average ionization potential of the stopping atoms. This formula is not readily applicable at low energies without correction terms which take into account the lesser influence of the inner atomic electrons on the stopping phenomenon. The dependence of ϵ on z^2 for particles of the same velocity, however, is probably valid down to the energies where capture and loss of electrons in the stopping material become important (around 300 kev for protons). It follows therefore that

$$\epsilon_p(E_p) = \frac{1}{4}\ \epsilon_\alpha(E_\alpha = 4E_p) \qquad \text{(IV-2)}$$

Estimates of ϵ_p (Li) based on eq. IV-2 were made from Rosenblum's[4] ϵ_α(Li) for E_α between 3 and 9 Mev. The lowest figure so obtainable was for E_p = 750 kev, while our data went up to 600 kev. The two curves do however appear to continue each other quite smoothly (fig. 11).

The curves given by Haworth and King[5], and by Warters[6],[7], lie about 10% above ours. The shapes of these curves agrees with ours within experimental error. The discrepancy in normalization is attributed to these authors' assumption of the validity of Bethe's formula (eq. IV-1) at low energies, and their consequent use of an average value of I as calculated by Mano[8] from Rosenblum's data. But our own calculations from Rosenblum's data have yielded values of I ranging continuously from 69 ev at E_α = 3 Mev down to 27 ev at E_α = 9 Mev. Values of I (ev) from our data for the various elements investigated are given below to show the unreliability of the formula in the low energy range:

E(kev)	Li	Be	Cu	Au	Pb
200	63.7	70.4	225	289	280
300	57.4	71.8	264	371	360
400	57.4	71.6	283	446	433
500	59.2	70.0	292	513	498
600	68.5	68.9	288	580	556

Around 340 Mev, where the formula is more reliable, the values of I (ev) are[3]: Li, 34; Be, 60; Cu, 300; Pb, 812; and Au at 18 Mev yields I = 1383 ev.

Beryllium (figs. 12, 13): The present curve for ϵ(Be) lies above Warshaw's[9] by about 15%. The shapes of the two curves are in fair agreement (fig. 13). The current relative measurements of F. Mozer[22] agree with ours from 200 to 600 kev. From 600 to 1800 kev, and with our normalization, Mozer's data falls from 6 to 3% above that of Kahn[11] and Madsen[10],[12]. The differences in the shapes of these various curves are within experimental error.

The foils used here for normalization had a density of about 0.224 mg/cm^2, and an area of 2.55 cm^2 (0.704" dia.) was accurately measured and weighed. The shape of the curve was checked by our own relative measurements below 250 kev and those of Mozer above 200 kev using a layer of 8 - 10 kev of evaporated Be on a gold target. Warshaw's foils had a density of 0.045 mg/cm^2, which would make them about 20 kev thick and hence quite suitable for energy loss measurements. We question, however, two points in his procedure: 1) such thin foils are available only in very small areas, which Warshaw measured by tracing their contour on gravimetric paper; it is felt that more error than the 1.5% which he claims may be involved; and 2) he did not perform his density determination on the same foil that he used for the energy loss determination, but on a foil evaporated at the same time; while this procedure is usually valid, it is conceivable that a considerable variation may have been present in an individual case.

Warshaw gathered considerable confidence in his results from the fact that his curve joined fairly smoothly the higher energy data of Madsen and Venkateswarlu[12]. It must be pointed out that this is true only if he passes his curve through his highest energy point, neglecting the previous one (fig. 13); but in that case, the shape of his curve no

longer agrees with ours and Mozer's in that region. It is his highest point, and not the previous, which Warshaw should have overlooked in drawing his curve.

Copper (figs. 14, 15): Between 400 and 600 kev, the slope of our relative measurements agrees with the data from Ohio State[13],[14]. Our normalization is however 3% higher; this brings it into better agreement with the data of Kahn[11], whose points however show considerable spread (fig. 15). Below 300 kev, our data is in fair agreement with that of Warshaw[8]. All of the above discrepancies are within the combined probable errors of the various curves. Madsen's data[10] are however 15% below these other measurements. This discrepancy can be attributed to his use of commercial rolled foils. Wilcox[16] has shown that an error of this magnitude can be explained in the case of commercial gold foils by the non-uniformity of these foils. Warshaw's normalization depended on the assumption that the density of the evaporated layer of copper was the same as the ordinary bulk density of the metal. The comparison of his results with ours tends to justify this assumption, which was not necessary in our experiment. In view, however, of the following discussion on gold, this agreement may be fortuitous.

Gold (figs. 16, 17): The present data on gold is in excellent agreement with the recent unpublished work of Ohio State[14] between 400 and 600 kev where the measurements overlap. We made absolute measurements with four distinct foils, and with mean energies lying between 320 and 340 kev. There was less than 1% spread from a mean curve through them (fig. 16). At lower energies the discrepancy with other observers reaches as much as 25% (fig. 17). In most cases, this can be attributed,

as explained above, by non-uniformity of the foils used. In the case of Warshaw's data another explanation is in order: as for his copper data, he measured evaporated foil thicknesses interferometrically and converted to areal density by using the bulk density of the metal. There is, to our knowledge, no experimental check of the validity of this assumption, except as may be implied by the above-mentioned data on copper. We note that all previous measurements are lower than ours and Ohio State's, rather than randomly distributed about these later ones. The reason for this is not clear.

Lead (figs. 18, 19): Our results for lead are in excellent agreement with those of Ohio State[14] above 400 kev. These in turn are in excellent agreement above 750 kev with α-particle data from Rosenblum[4], as calculated from eq. IV-2.

LiF and CaF_2 (figs. 20, 21): Since no measurements have been previously published on LiF and CaF_2, no comparison is possible. Three absolute determinations were made on each, near 350 kev, and relative values were obtained between 50 and 600 kev. The internal consistency of the data is excellent, with two or three points at the low energy end falling some 2.5% away from a smooth curve fitting the data.

The molecular stopping power of a compound can, to a first approximation, be taken as the sum of the atomic stopping powers of its constituent elements. This simple rule is known as Bragg's law, and has been extensively discussed by Platzman[23]. Its limitations can be traced to three sources: 1) the excitation energies of the molecular system may be quite different from those of the atomic system; Platzman

estimates that the deviations from Bragg's law due to this effect cannot exceed 5%; 2) the incident particles may excite rotational and vibrational modes of the molecules; Platzman shows that this is unimportant down to 300 kev, where about 1% of the energy loss may be contributed in this way; and 3) in the case of solids, where the molecules are very close together, intermolecular forces may come into play and these are not currently understood quantitatively. Platzman does point out, however, that unusual effects may be expected from C, N, O, and F, because these elements form many different types of bonds in compounds.

With these restrictions in mind, a curve has been calculated for fluorine by subtracting the lithium data from the lithium fluoride curve. The resulting data for 1/2 F_2 is shown in fig. 22, where the data of Reynolds[24],[25] for the neighboring atoms $\frac{1}{2}$ O_2 and Ne is plotted for comparison. In view of the above discussion, this curve has little reliability below 300 kev. Since the binding in LiF does not have the unusual features present in, say, a benzene ring, it is probably safe to say that the 1/2 F_2 curve is good to $\pm$ 5% above 300 kev. Since a direct measurement is rendered experimentally difficult by the high reactivity of fluorine, this is the best that can be done at the present; and it is probably valid for the computation of ϵ in other compounds where the binding is of a simple type, as opposed to a resonant structure.

V. ERRORS

We reproduce here for convenience eq. II-5 which gives the stopping cross section in terms of the experimentally measured quantities:

$$\epsilon(E) = \frac{M}{N_o} \frac{A}{W} \Delta E \cos \theta \qquad (V\text{-}1)$$

where A, W, M are the area, weight, and atomic (molecular) weight, respectively, of the evaporated deposit; ΔE is the energy lost in the deposit; θ is the angle from the normal at which the beam goes through the foil; and N_o is Avogadro's number.

The upper limits on the errors in the determination of ϵ were as follows:

W/A (Chem.)	1.7%	cos θ	0.06%
A	1.0%	E	0.75 - 1.5%
W	0.9%	ΔE	1.9 - 2.4%

Impurities in materials used: 0.005 to 1.0%

As can be seen from this summary, the errors in the determination of energy losses were by far the largest, and were the limiting factor in the overall accuracy of the experiment. The details of these sources of error and their values are discussed below.

Impurities: As can be seen from Table III, the possible amounts of impurity originally present are well under 1%, except in the case of lithium. As can be seen from the scattering analysis, figure 3, the amounts of impurity in our sample of lithium were also considerably under 1%. The only data on beryllium is the scattering analysis,

figure 6; it was shown in section II that the value of ϵ was not measurably affected by the impurities present.

Areas: The measurements of area with the traveling microscope had an accuracy of 1% or better. Predictions made from geometry agreed with these to within a few tenths of one percent.

Weights: As described in section III, the standard weights were reliable to 0.5%. The uncertainty in reading the angles from the vernier was 1/2 min. The individual settings varied by ± 1 min. from the average, because of the coarseness of the fiber and the cross-hair in the telescope. The probable error in an average of three readings was then 0.58 min. The composite angular uncertainty for a difference of two weighings was then ± 1.1 min. The sensitivity of the fiber was, typically, 2.6 μg/min., so that the angular error corresponded to ± 2.9 μg. The smallest weight difference was 400 μg, so that in the worst case we had a 0.75% angular uncertainty in addition to the 0.5% uncertainty in calibration. Hence the weight differences were known to better than 0.9%. The stability of the weights of the foils was checked as described in section III, part 2; no changes in weight were ever detected.

W/A (Chemical Method): An acid-base titration is a very simple experiment which, with proper precautions, can be performed very accurately. The standard used was 0.1000 ± 0.0002 N HCl, as furnished by the Braun Corporation, Los Angeles. The indicator used was brom-phenol blue, whose color change is slightly on the acid side. This was done, upon advice of the Chemistry Department, to eliminate the effect of possible carbonates in the solution. End point corrections were of course made.

Small errors (under 1%) were involved in reading the burette. The geometry of the evaporation was known to 1%. As discussed in part II, an additional error of 1% is possible in the application of the correction to eq. II-4 for the density of the deposit. The composite error in W/A is then 1.7%. We note here that we do not know whether the lithium was deposited at the same rate on the thin aluminum foil as on the tantalum collector. This, incidentally, provided one of the incentives for developing the micro-balance method, in which all measurements were made on the same thin aluminum foil. The excellent agreement between the results of the two methods indicates that the assumption of the equal rates of deposition was justified.

cos θ: The angle at which the beam passed through the aperture in the foil holder was $14.1 \pm 0.25^{\circ}$ (fig. 7). As must be clear from the description of the way the foils were held (sect. III part 3, and fig. 7), they could not always be kept strictly parallel with the holder. This effect, together with a small amount of curvature in some foils, was estimated to give an uncertainty of $\pm 1^{\circ}$. The angular spread of the beam was 5°, so that we may take a 1° possible error in using the mean value. Combining these errors, we get $\theta = 14.1 \pm 1.45^{\circ}$, or

$$\frac{d \cos \theta}{\cos \theta} = \tan \theta \, d\theta = 0.064\%$$

Energies and energy losses: Any energy value is the product of the electrostatic analyzer calibration constant by the voltage between the analyzer plates (as measured by the voltage drop across a resistor in a standard potentiometer circuit). The analyzer was calibrated to $\pm$ 0.5% against the well established resonance in $F^{19} + p$ at 340.4 kev[26].

The positions of the gold steps were taken as half way up the steps (fig. 1). This procedure is justified if the statistical distributions of the straggling and the energy loss are Gaussian, or at least symmetric about the mean; in this case one gets the mean values of the energy losses. The symmetry of the curves obtained tends to justify these assumptions, and no error has been included for their uncertainty. The clean gold steps were quite sharp with a very flat top (fig. 1), so that the uncertainty in determining their midpoint was always less than 0.3% of ΔE. With a foil and deposit in the path of the beam, however, the greater slope of the step meant a greater uncertainty in the midpoint. This was aggravated by the fact that with a thick deposit, more spread was observed in the points determining the top, as well as in the points on the step itself. This effect was particularly marked at low energies. For these reasons, an uncertainty of 1.5% of ΔE was not uncommon above 150 kev, while 2% must be allowed below 150 kev. The values of $\Delta E/E$ were always 1/2 or smaller, so that the maximum errors in E due to the causes discussed in this paragraph were 0.75 to 1%.

An additional error was introduced by the small amount of drifting of the spectrometer field. This drifting never exceeded 2% of ΔE. Corrections were made whenever possible, as illustrated in section II, part 1. A 1% probable error is retained. In relative measurements, where the two gold steps needed were measured within 20 minutes of each other, the drift was negligible. In the cases of lithium and lead, drifts amounting to 3% of ΔE were occasionally observed because of the length of the experiment (see section II, part 2).

Combining these various probable errors yields uncertainties of 1.5% in E and 1.9 to 2.4% in ΔE.

The probable errors in ϵ: The probable errors in the absolute values were computed as the square root or the sum of the squares of the probable errors in the parameters used to compute ϵ (eq. V-1). This procedure yields 2.6% for the micro-balance method and 2.8% for the chemical method.

As read from a mean curve drawn through the data, relative values are subject to less random error than the individual measurements. An estimate of the errors can be made by drawing extreme curves which might conceivably fit the data. Thus the ends of the curves (here near 50 and 600 kev) may be in error by as much as the one or two points determining them. On the other hand, in regions where many experimental points must be fitted, there is less latitude for drawing a visually reasonable curve. From such an analysis, we arrive at probable errors of 2.5% from 50 to 100 kev and 1.8% from 500 to 600 kev, which are essentially the errors in ΔE in those ranges(relative values depend only on ΔE); and from 100 to 500 kev, one obtains from 1.8 to 1.3%.

These errors must of course be compounded with the normalization errors. The probable errors adopted for the experimental results as listed in tables I and II are then:

Absolute values (micro-balance)	2.6%
Absolute values (chemistry)	2.8%
Normalized relative values	
a) 50 - 100 kev	3.5%
b) 125 - 450 kev	3.0%
c) 500 - 600 kev	3.1%

The variations in error of individual values over the ranges involved are too small to warrant a finer subdivision. This is also the case for variations in different elements, though some were more difficult to handle than others. It is interesting to note how in the high energy range, the smaller error in ΔE compensates for the fact that few points determine the curve; at low energies, however, these errors are both large.

TABLE I

The Absolute Values of ϵ (10^{-15} ev - cm^2)

The probable errors are: for the first four numbers, obtained by the chemical method, ± 2.8%; and for the others, obtained by the weighing method, ± 2.6%.

Substance	ϵ	Energy (kev)
Lithium	4.60	441
	4.53	450
	4.56	430
	5.07	382
	4.75	416
	4.87	404
Beryllium	6.63	323
	5.14	518
Copper	20.5	344
	19.8	401
	19.7	380
Gold	34.8	335
	35.0	321
	35.0	330
	35.6	327
Lead	37.2	329
	36.5	353
Lithium Fluoride	16.8	358
	16.2	367
	16.1	379
Calcium Fluoride	43.7	331
	42.4	374
	43.5	352

TABLE II

ϵ (10^{-15} ev-cm^2) as read from the smooth curves through the relative measurements normalized to the values in Table I. Energies are in kev.

Energy	Li	Be	Cu	Au	Pb	LiF	CaF_2	LiF - Li
50		10.3	21.5	28.2		22.6	57.2	
75	8.45	10.5	23.0	31.7	39.4	25.3	66.2	(16.9)
100	8.70	10.45	24.0	34.5	41.6	26.3	69.0	(17.6)
125	8.35	10.2	24.3	36.6	43.0	25.8	68.6	(17.4)
150	7.72	9.80	24.0	37.9	43.7	24.2	65.2	(16.5)
175	7.25	9.27	23.4	38.6	43.9	22.4	61.6	(15.2)
200	6.90	8.73	22.9	38.8	43.6	21.0	57.8	(14.2)
250	6.35	7.75	21.8	38.2	41.7	19.2	50.7	(12.9)
300	5.83	7.03	21.0	36.4	39.0	17.9	46.0	12.1
350	5.28	6.44	20.2	34.0	36.5	16.7	43.3	11.4
400	4.88	5.98	19.5	31.6	34.4	15.6	40.8	10.7
450	4.50	5.58	18.9	30.0	32.3	14.4	39.1	9.9
500	4.17	5.25	18.3	28.5	30.6	13.5	37.8	9.3
550	3.78	4.96	17.9	27.3	29.2	12.7	36.6	8.8
600	3.53	4.69	17.5	26.3	28.0	12.2	36.0	8.5

The probable errors in this table are ± 3.5% from 50 to 100 kev; and ± 3.1% from 125 to 600 kev

TABLE III

Impurities In Substances Used

Substance	Source	Impurities Kind	Max. %
CaF_2	General Chemical Company	Cl	0.01
		SO_4	0.005
		Fe	0.02
		Other	0.01
LiF	General Chemical Company	Cl	0.01
		CO_3	0.01
		SO_4	0.01
		Ba	0.01
		K	0.1
		Na	0.2
		Other	0.01
Pb	J. T. Baker Chemical Company	Other metals	0.06
Cu	J. T. Baker Chemical Company	Other metals	0.02
Li	Lithium Corporation of America	K, Na	1.0
Au	Wildberg Bros. (Los Angeles)	Cu, Ag	0.005

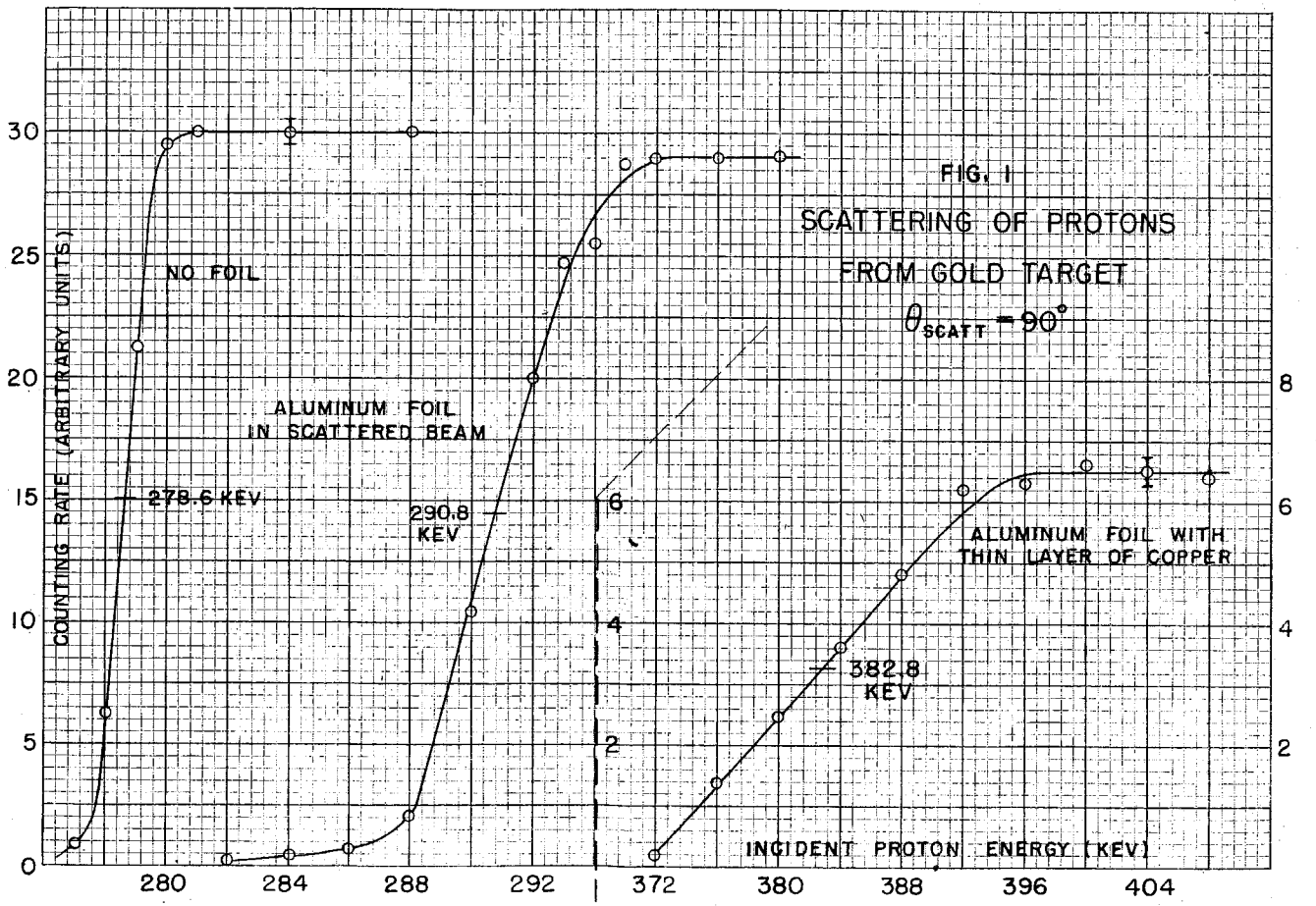

FIG. 2
EXPERIMENTAL ARRANGEMENT
CHEMICAL METHOD

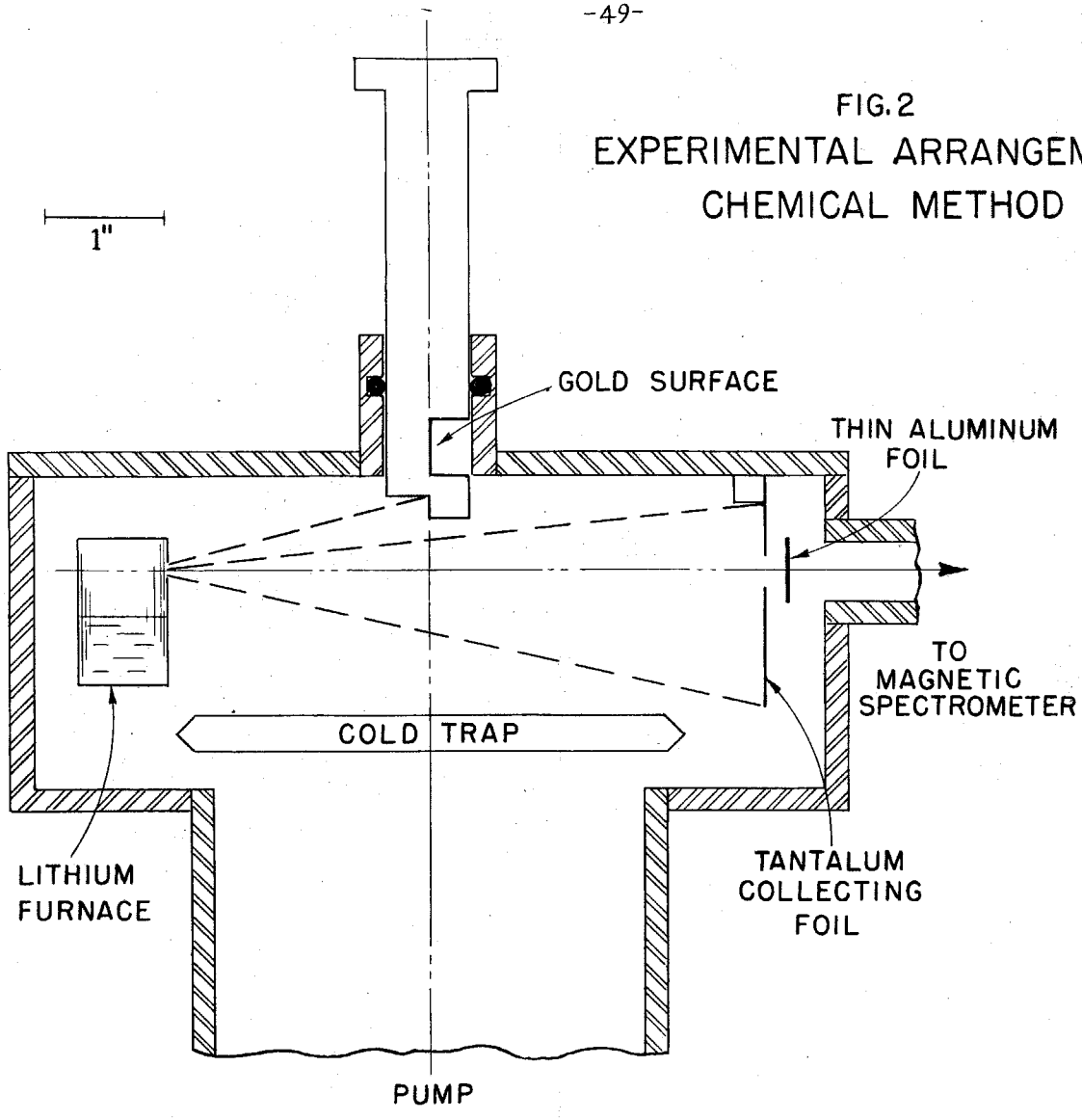

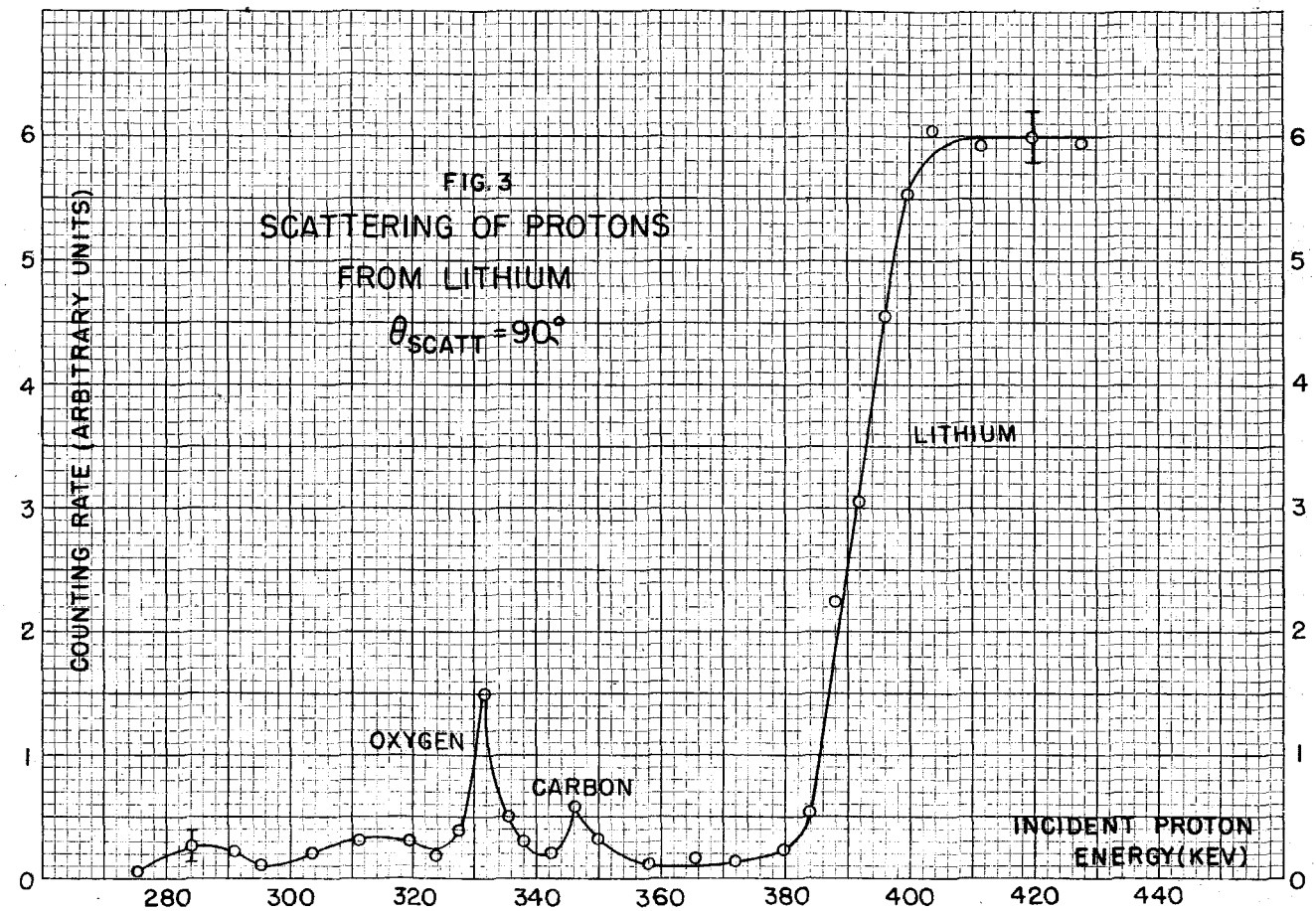

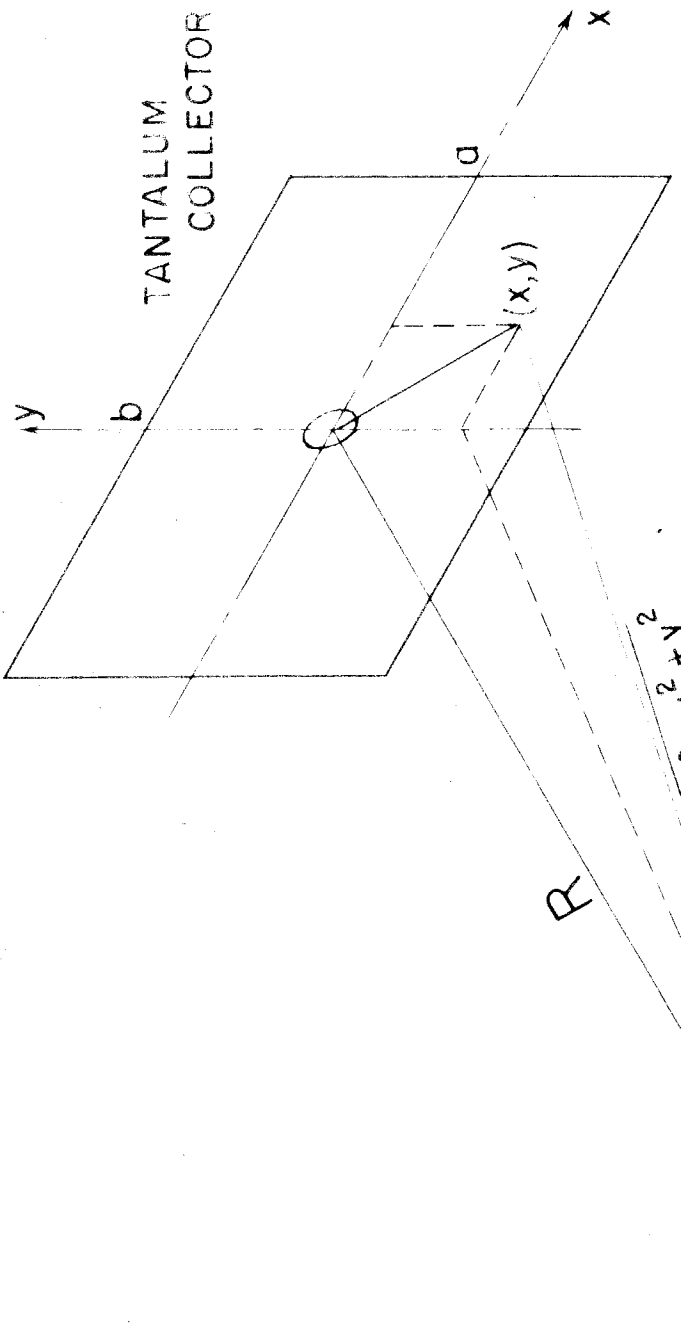

FIG.4

GEOMETRY OF THE
LITHIUM EVAPORATION

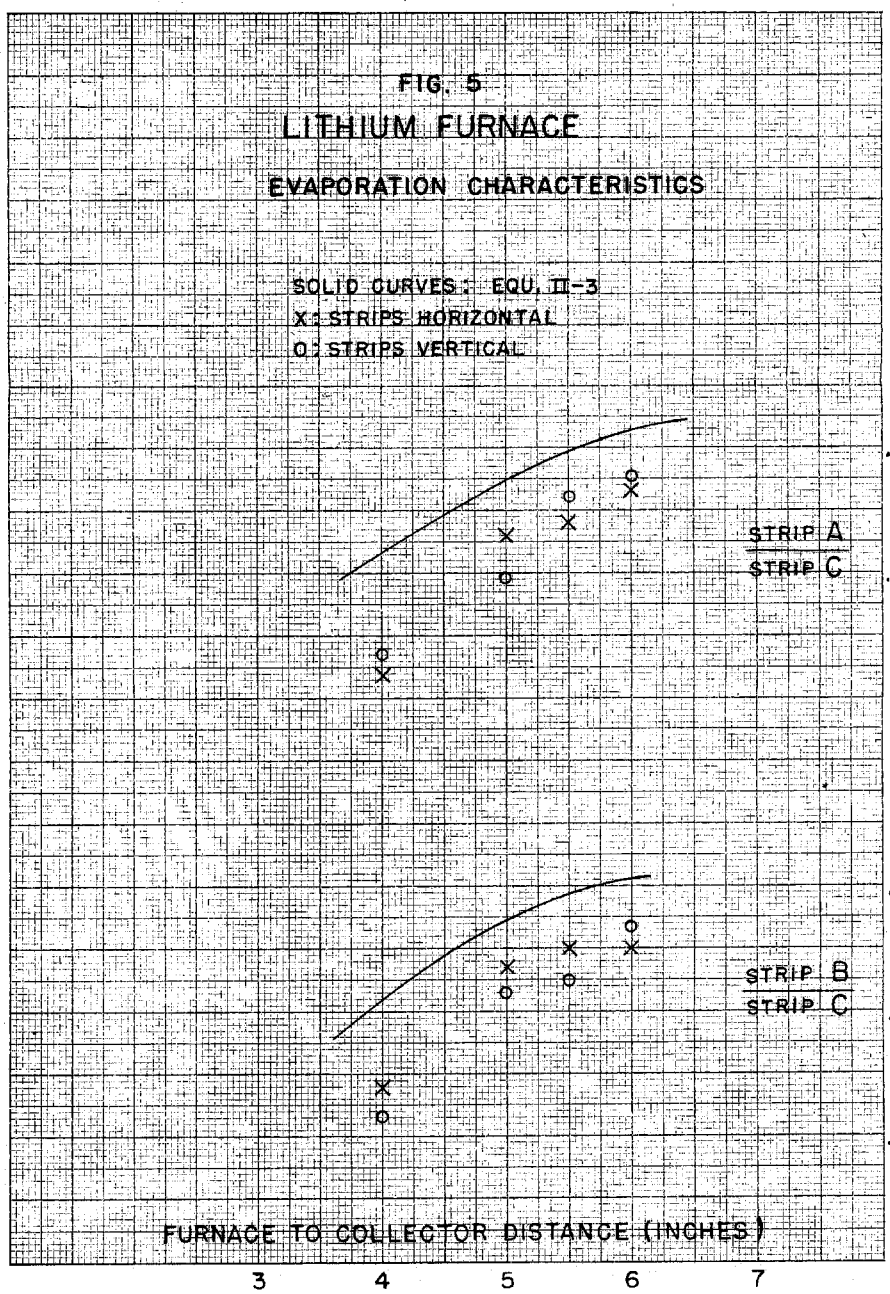
FIG. 5
LITHIUM FURNACE
EVAPORATION CHARACTERISTICS
SOLID CURVES: EQU. II-3
X: STRIPS HORIZONTAL
O: STRIPS VERTICAL
STRIP A / STRIP C
STRIP B / STRIP C
.950
.900
.850
.950
.900
.850
FURNACE TO COLLECTOR DISTANCE (INCHES)
3
4
5
6
7

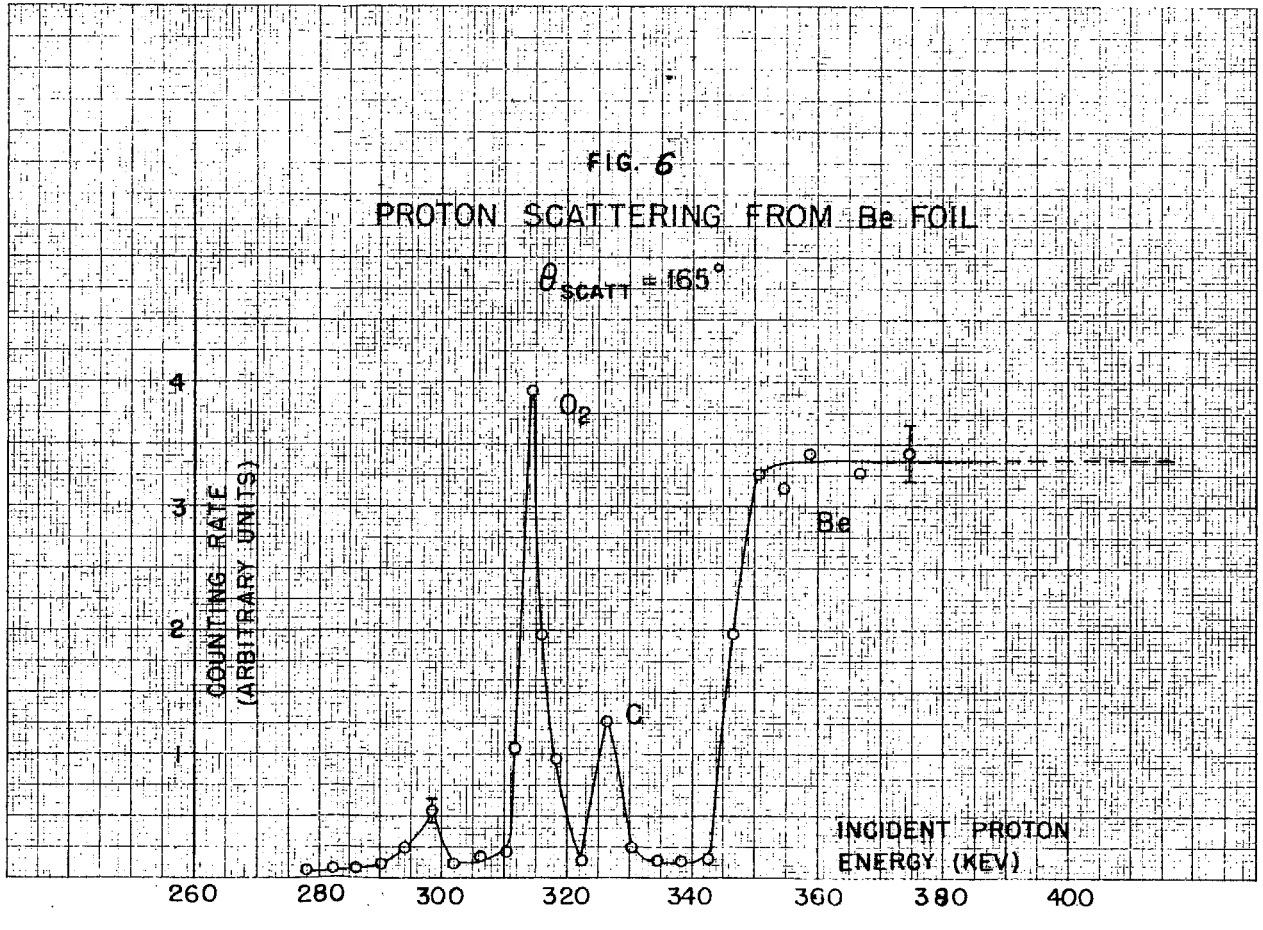
FIG. 6
PROTON SCATTERING FROM Be FOIL
$\theta_{SCATT} = 165°$
COUNTING RATE (ARBITRARY UNITS)
1
2
3
4
O_2
C
Be
INCIDENT PROTON ENERGY (KEV)
260
280
300
320
340
360
380
400

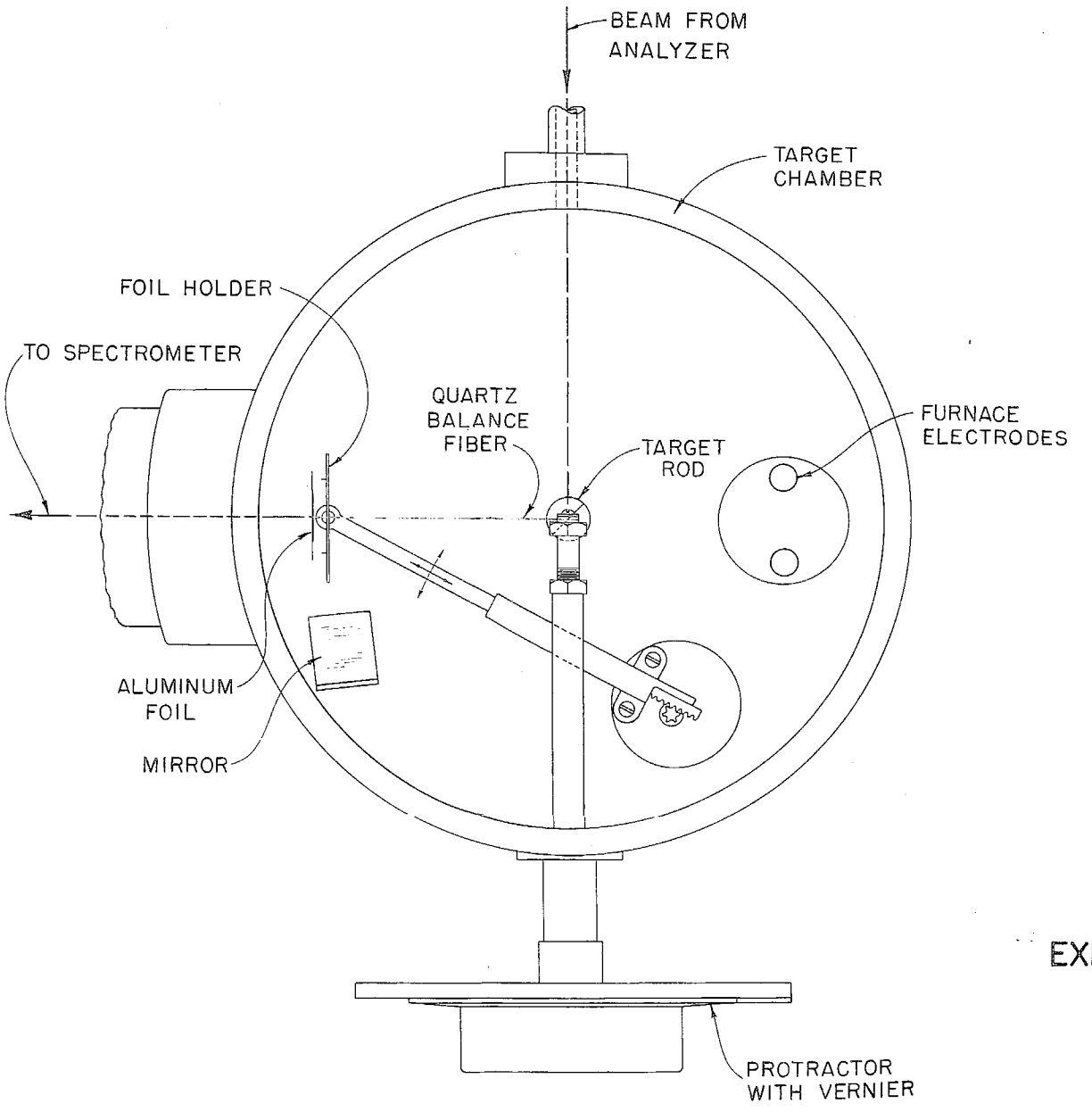

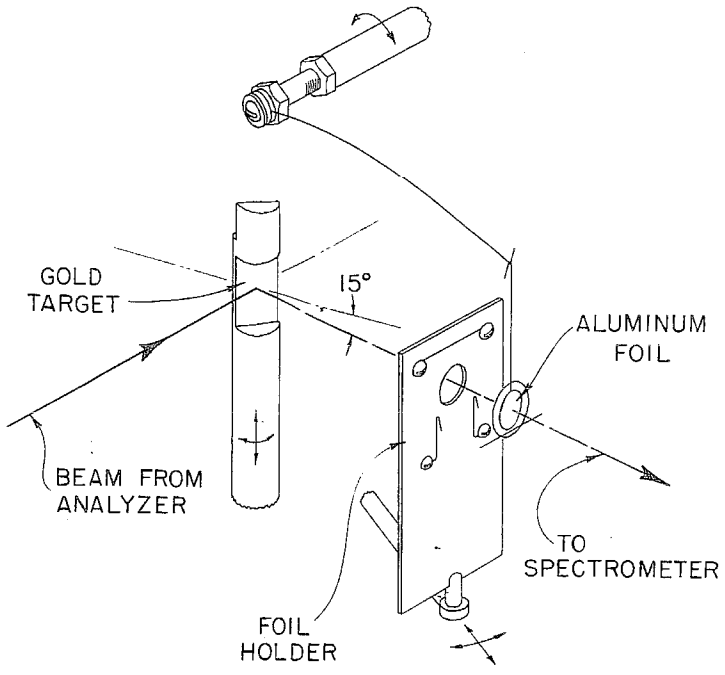

EXPERIMENTAL ARRANGEMENT
WEIGHING METHOD

FIG. 7

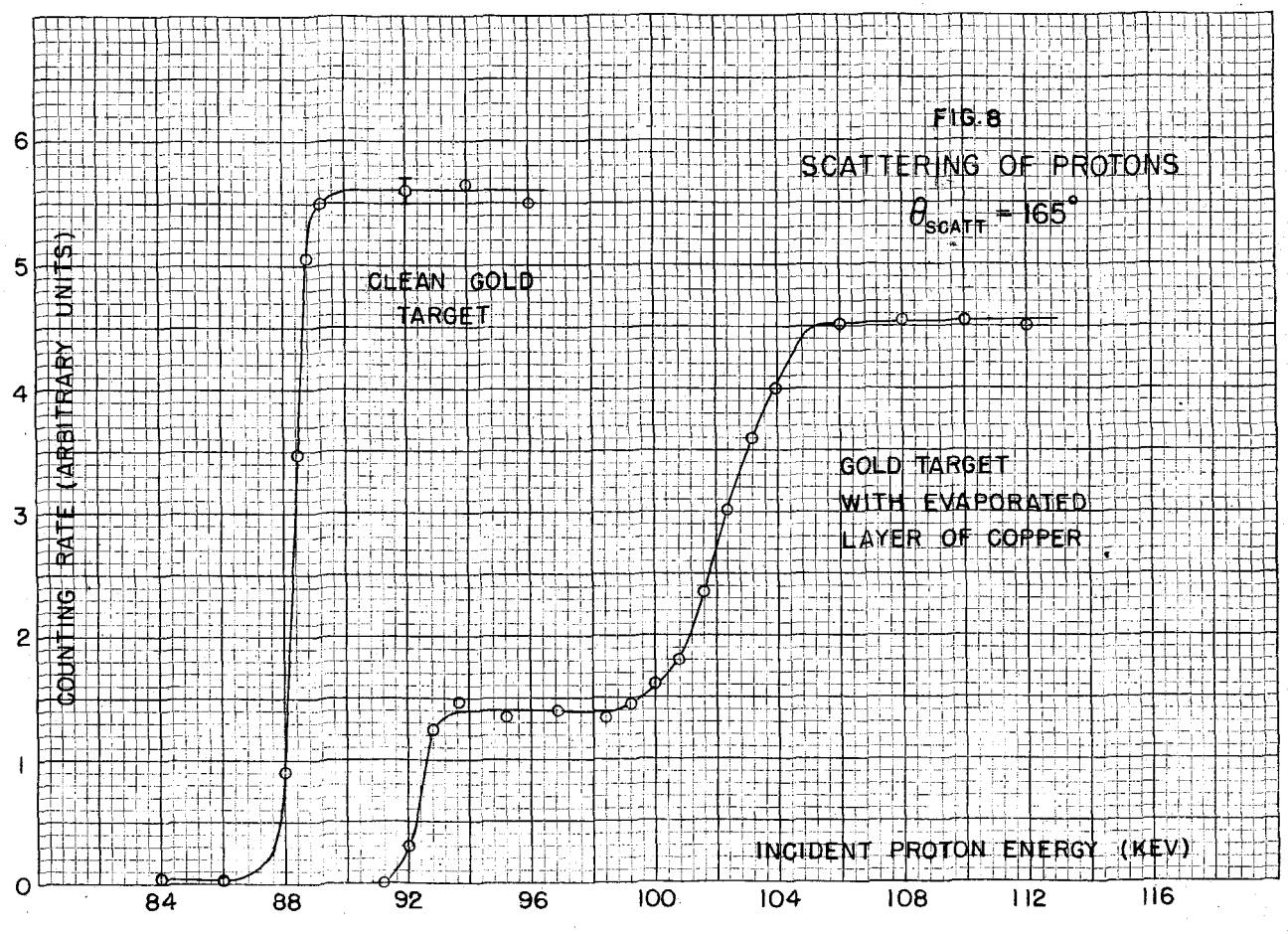

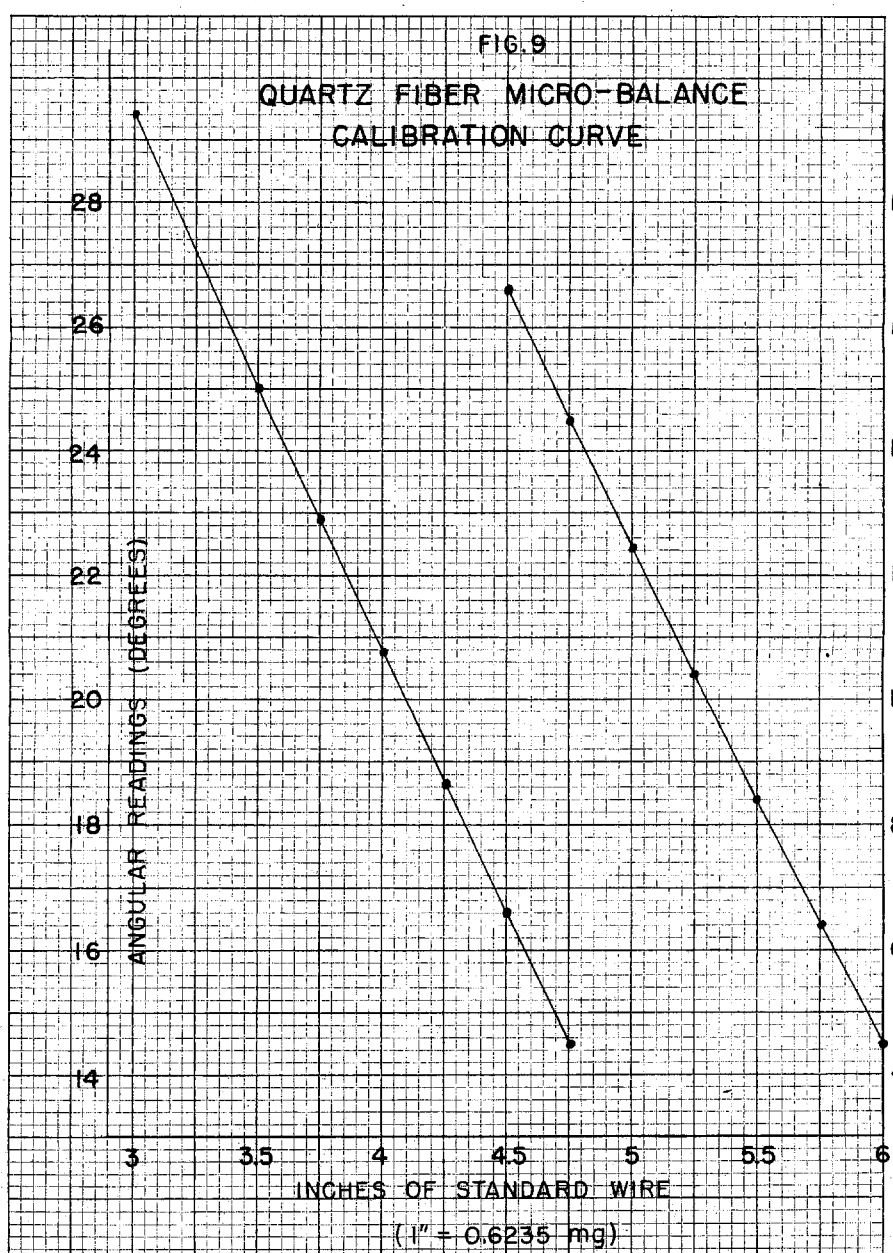

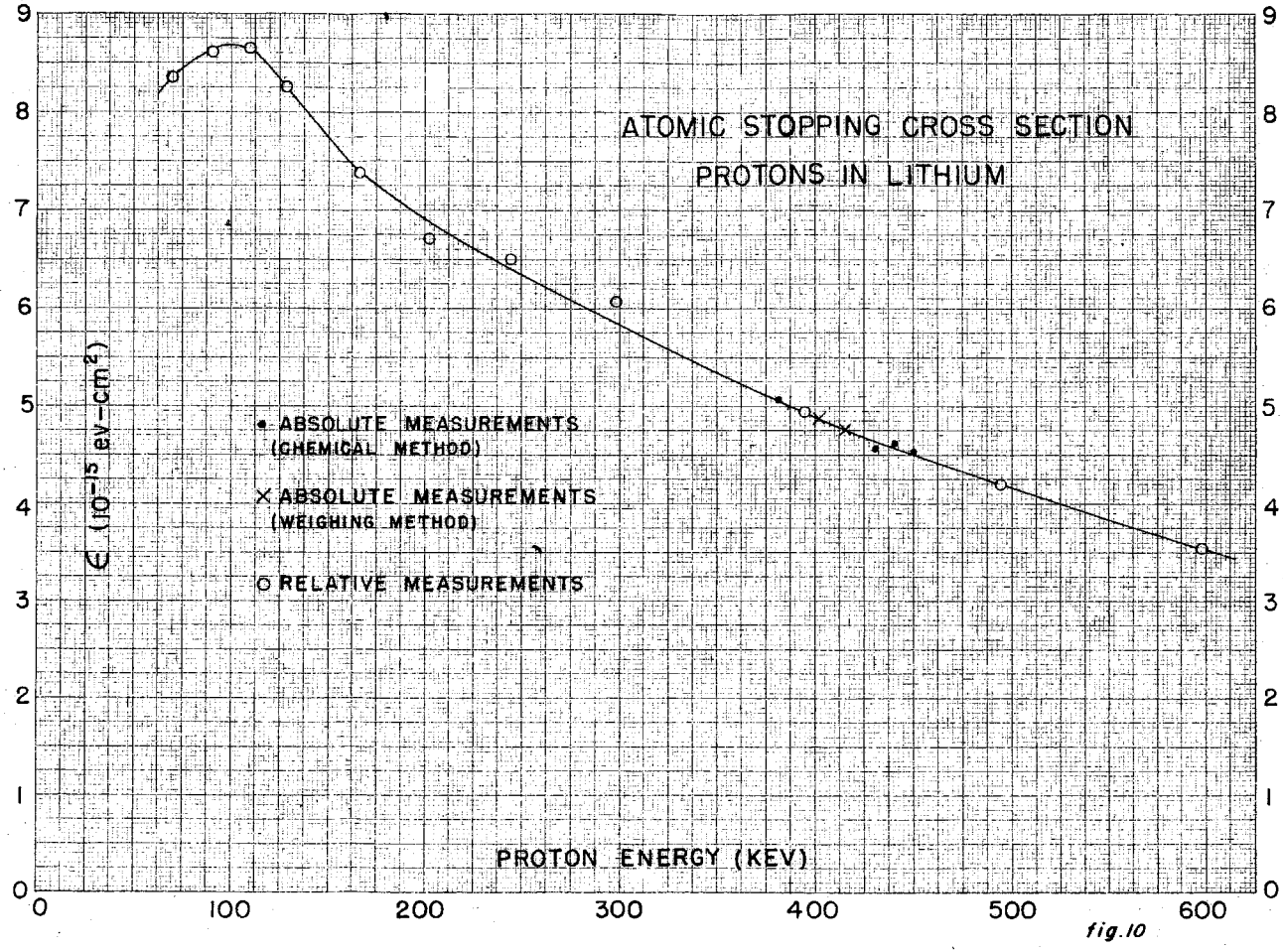
ATOMIC STOPPING CROSS SECTION
PROTONS IN LITHIUM
ε (10⁻¹⁵ ev-cm²)
• ABSOLUTE MEASUREMENTS (CHEMICAL METHOD)
× ABSOLUTE MEASUREMENTS (WEIGHING METHOD)
○ RELATIVE MEASUREMENTS
PROTON ENERGY (KEV)
0
1
2
3
4
5
6
7
8
9
0
100
200
300
400
500
600

fig.10

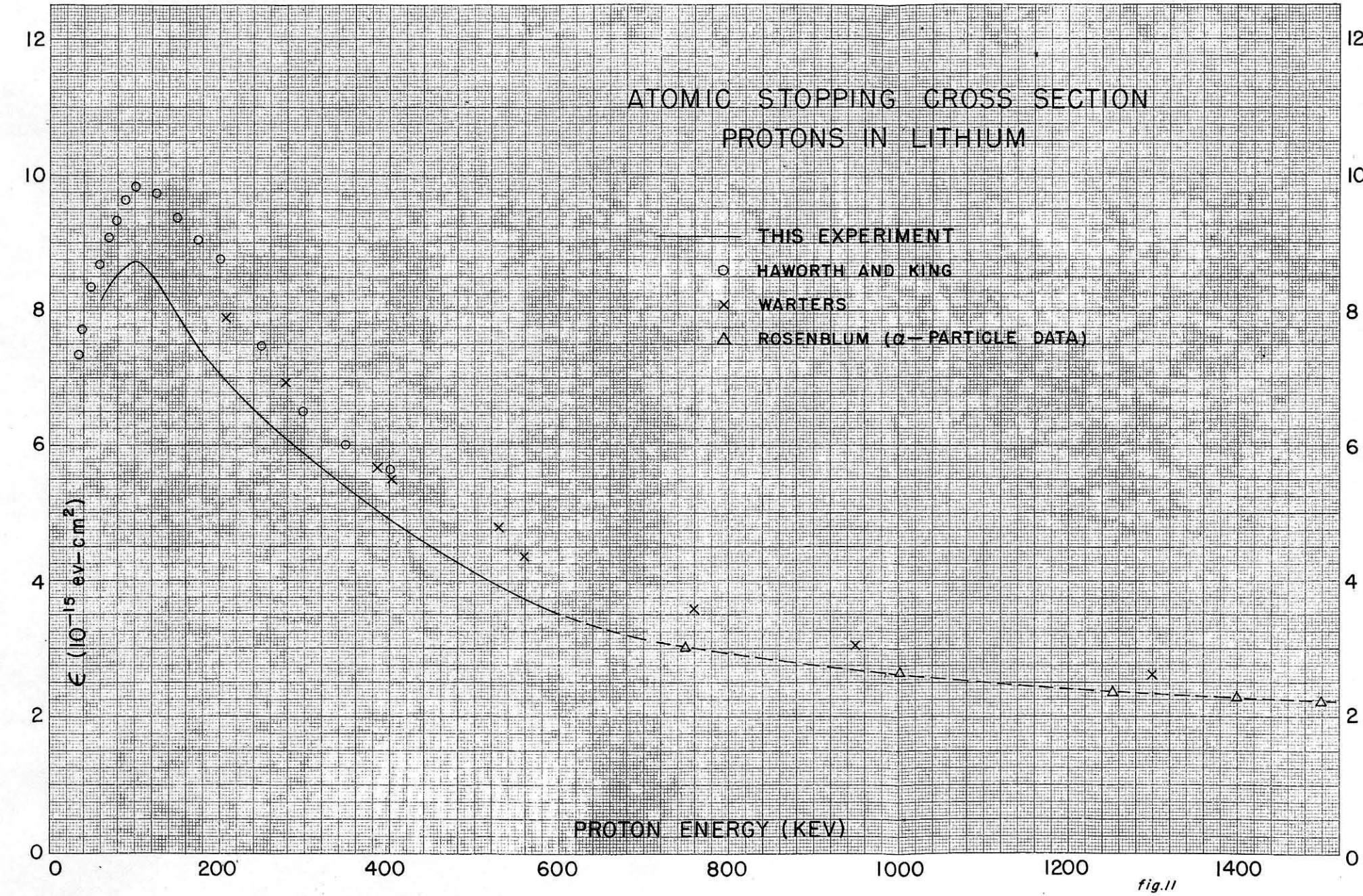
ATOMIC STOPPING CROSS SECTION
PROTONS IN LITHIUM
THIS EXPERIMENT
HAWORTH AND KING
WARTERS
ROSENBLUM (α — PARTICLE DATA)
ε (10⁻¹⁵ ev-cm²)
PROTON ENERGY (KEV)
0
2
4
6
8
10
12
0
200
400
600
800
1000
1200
1400

fig.11

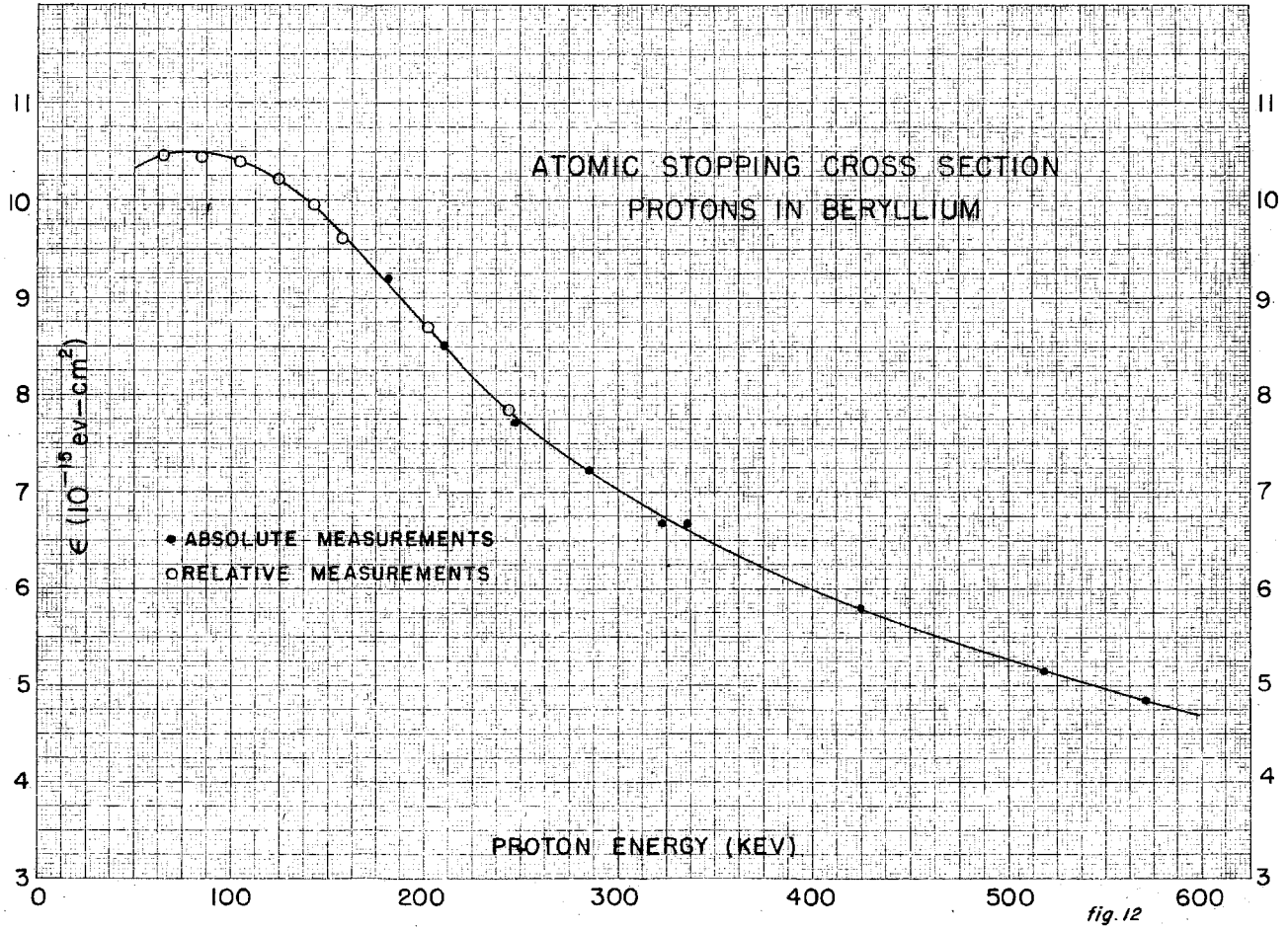
ATOMIC STOPPING CROSS SECTION
PROTONS IN BERYLLIUM
ε (10⁻¹⁵ ev-cm²)
● ABSOLUTE MEASUREMENTS
○ RELATIVE MEASUREMENTS
PROTON ENERGY (KEV)
0
100
200
300
400
500
600
3
4
5
6
7
8
9
10
11

fig. 12

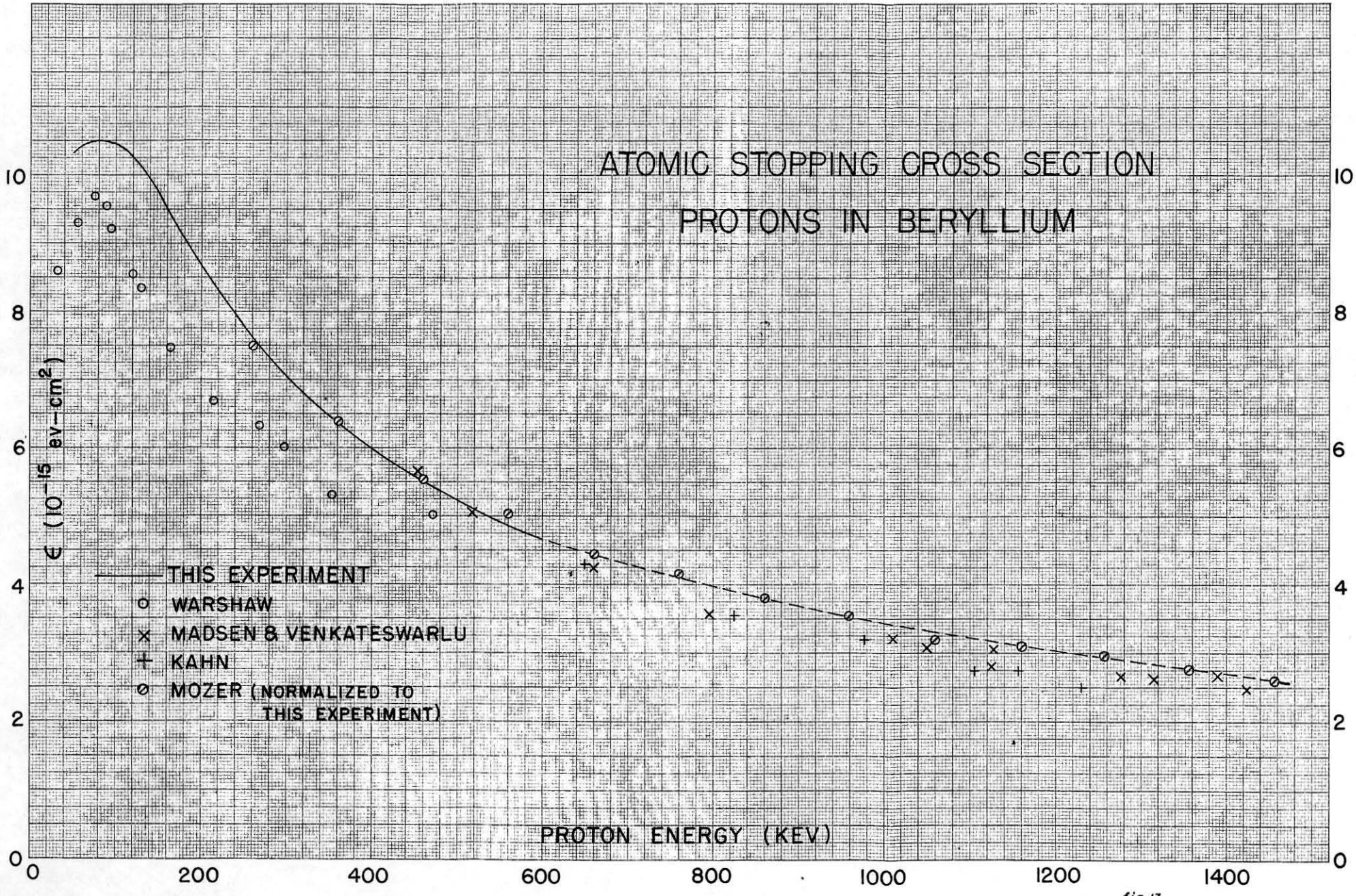
ATOMIC STOPPING CROSS SECTION
PROTONS IN BERYLLIUM
ε (10⁻¹⁵ eV-cm²)
PROTON ENERGY (KEV)
THIS EXPERIMENT
WARSHAW
MADSEN & VENKATESWARLU
KAHN
MOZER (NORMALIZED TO THIS EXPERIMENT)
0
2
4
6
8
10
0
200
400
600
800
1000
1200
1400

fig. 13

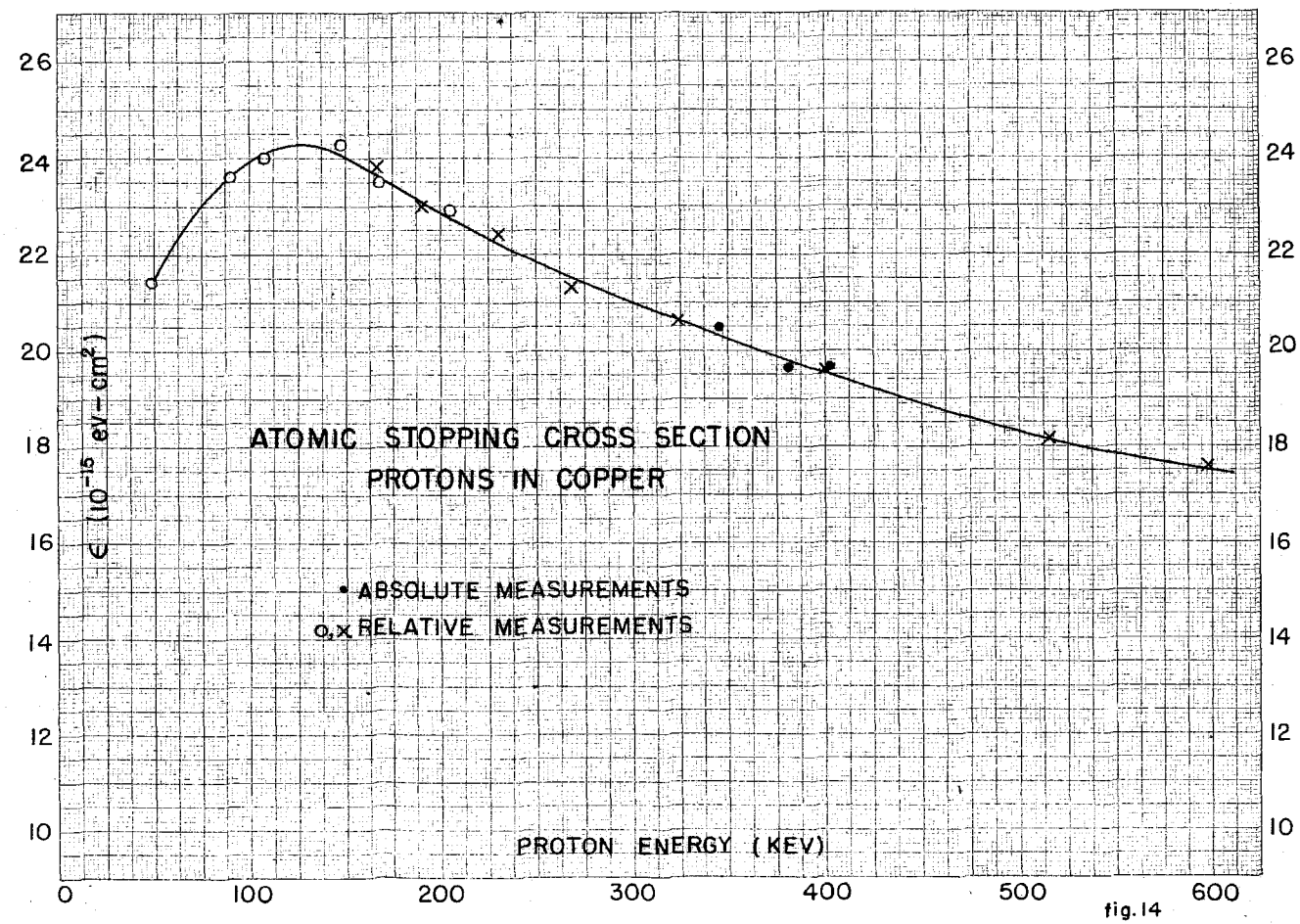
ATOMIC STOPPING CROSS SECTION
PROTONS IN COPPER
• ABSOLUTE MEASUREMENTS
o, x RELATIVE MEASUREMENTS
ε (10⁻¹⁵ eV - cm²)
PROTON ENERGY (KEV)
26
24
22
20
18
16
14
12
10
0
100
200
300
400
500
600

fig. 14

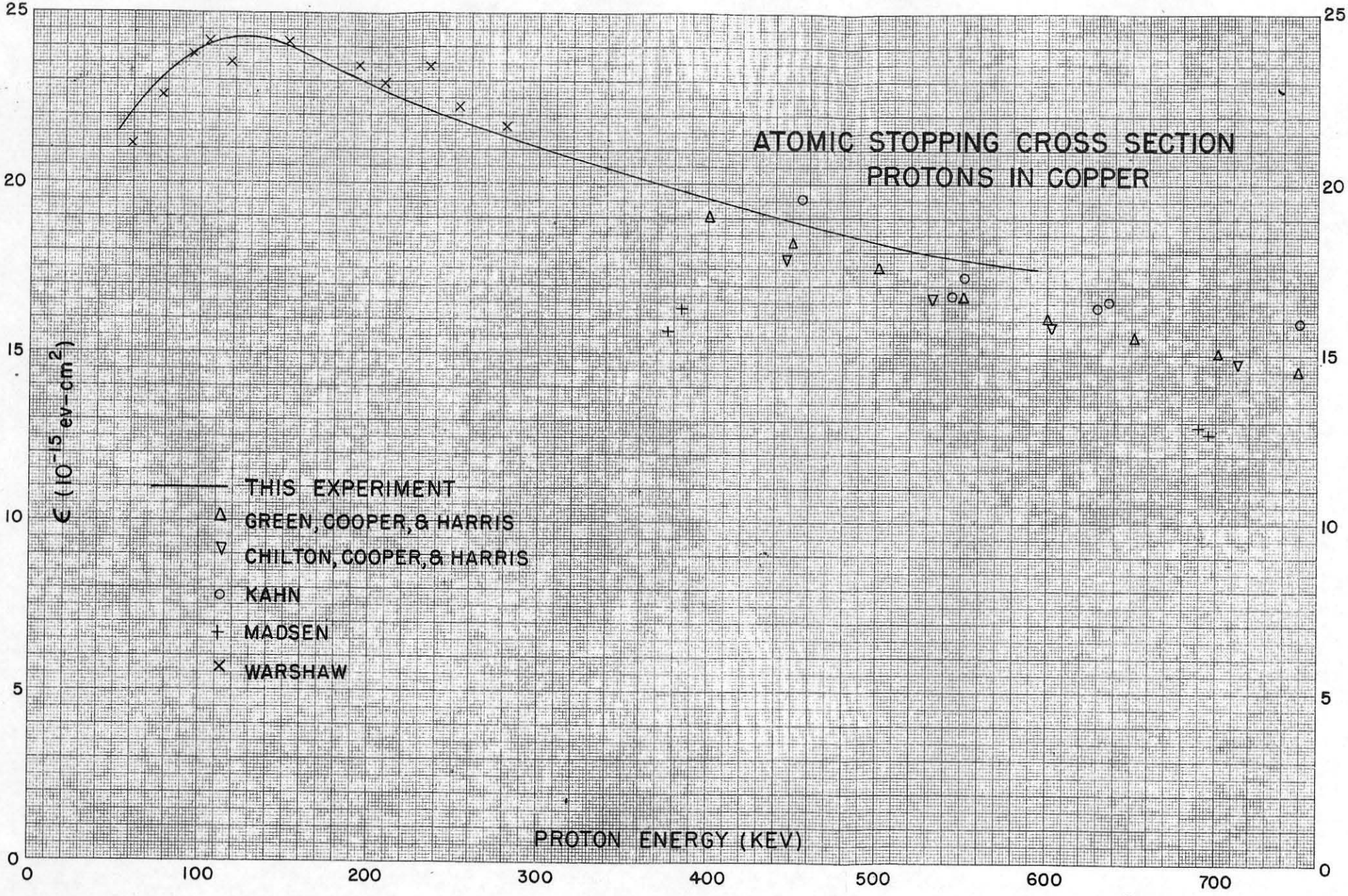
ATOMIC STOPPING CROSS SECTION
PROTONS IN COPPER
ε (10⁻¹⁵ ev-cm²)
PROTON ENERGY (KEV)
THIS EXPERIMENT
GREEN, COOPER, & HARRIS
CHILTON, COOPER, & HARRIS
KAHN
MADSEN
WARSHAW
0
5
10
15
20
25
0
100
200
300
400
500
600
700

fig. 15

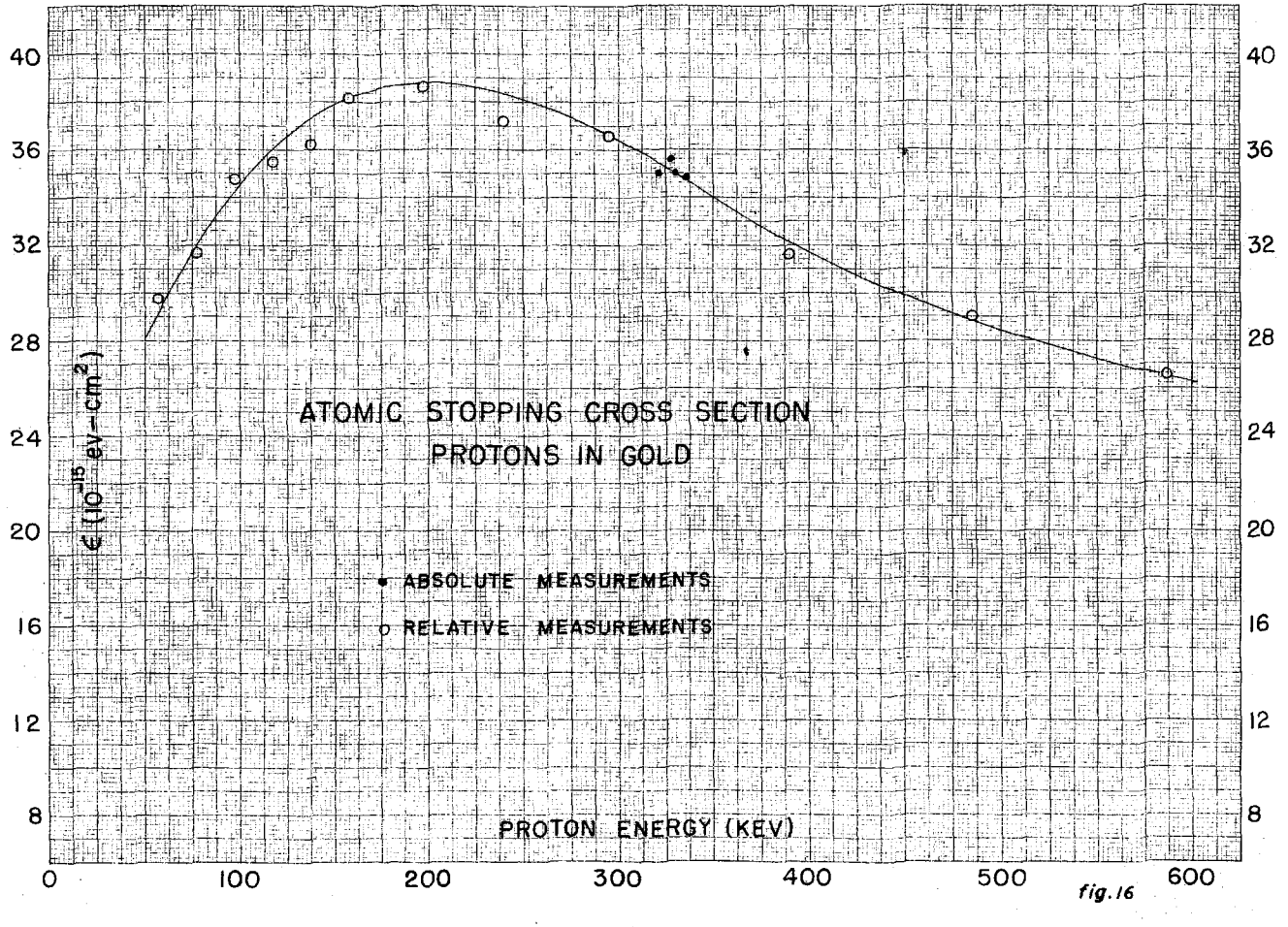
ATOMIC STOPPING CROSS SECTION
PROTONS IN GOLD
ε (10⁻¹⁵ ev-cm²)
• ABSOLUTE MEASUREMENTS
○ RELATIVE MEASUREMENTS
PROTON ENERGY (KEV)
40
36
32
28
24
20
16
12
8
0
100
200
300
400
500
600

fig. 16

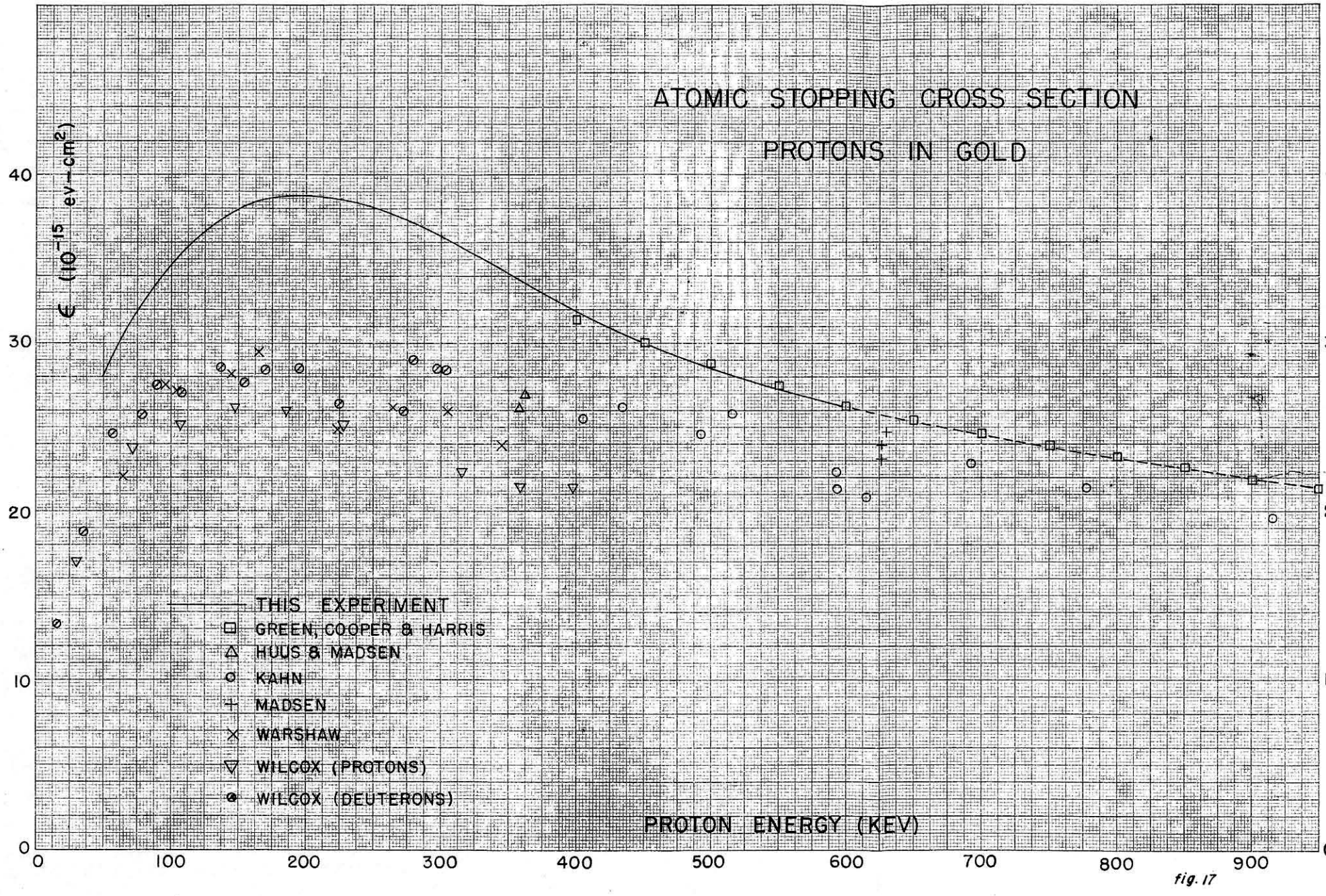
ATOMIC STOPPING CROSS SECTION
PROTONS IN GOLD
ε (10⁻¹⁵ ev-cm²)
PROTON ENERGY (KEV)
THIS EXPERIMENT
GREEN, COOPER & HARRIS
HUUS & MADSEN
KAHN
MADSEN
WARSHAW
WILCOX (PROTONS)
WILCOX (DEUTERONS)
0
10
20
30
40
0
100
200
300
400
500
600
700
800
900

fig. 17

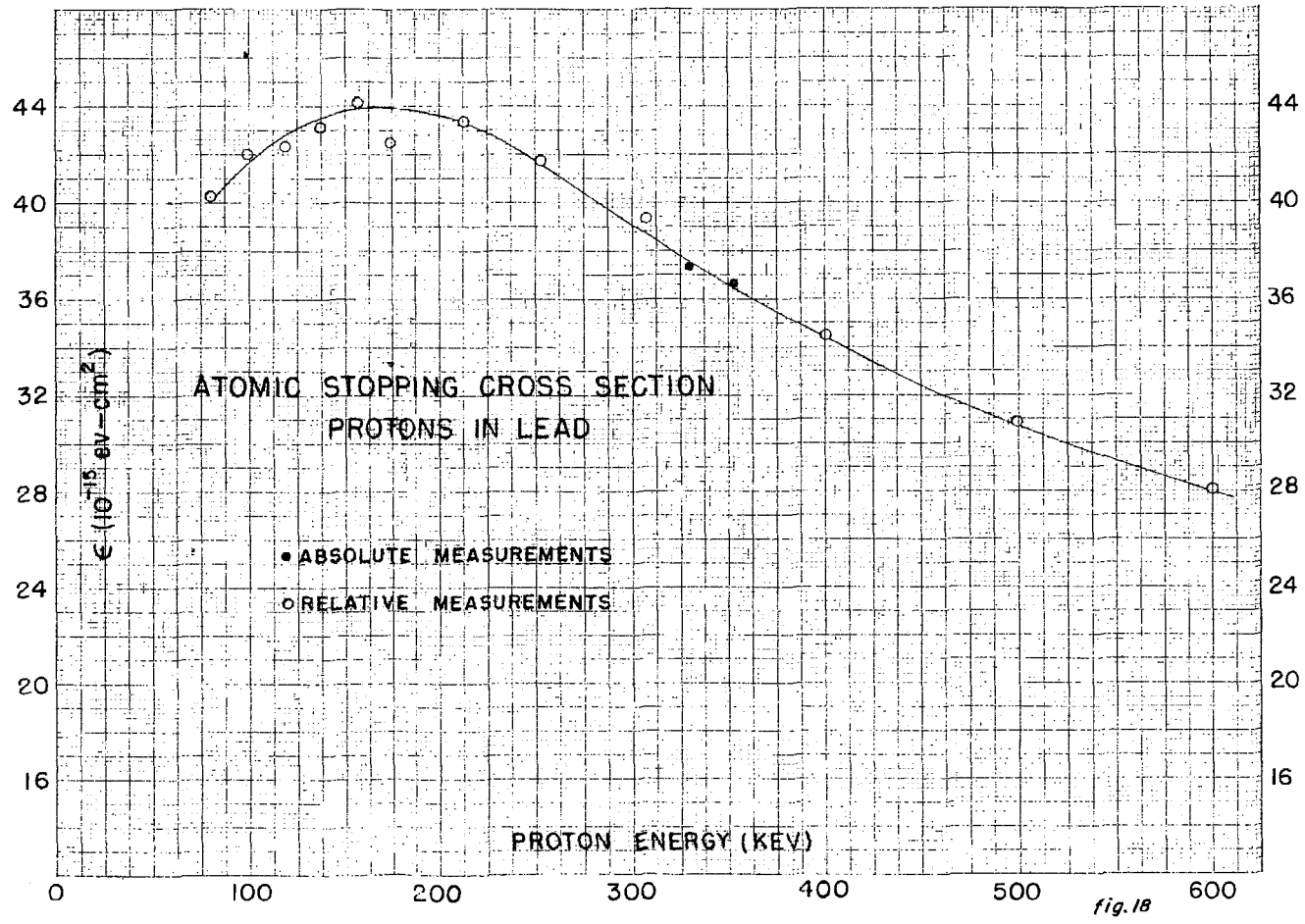
ATOMIC STOPPING CROSS SECTION
PROTONS IN LEAD
• ABSOLUTE MEASUREMENTS
○ RELATIVE MEASUREMENTS
ε (10⁻¹⁵ ev-cm²)
PROTON ENERGY (KEV)
44
40
36
32
28
24
20
16
0
100
200
300
400
500
600

fig. 18

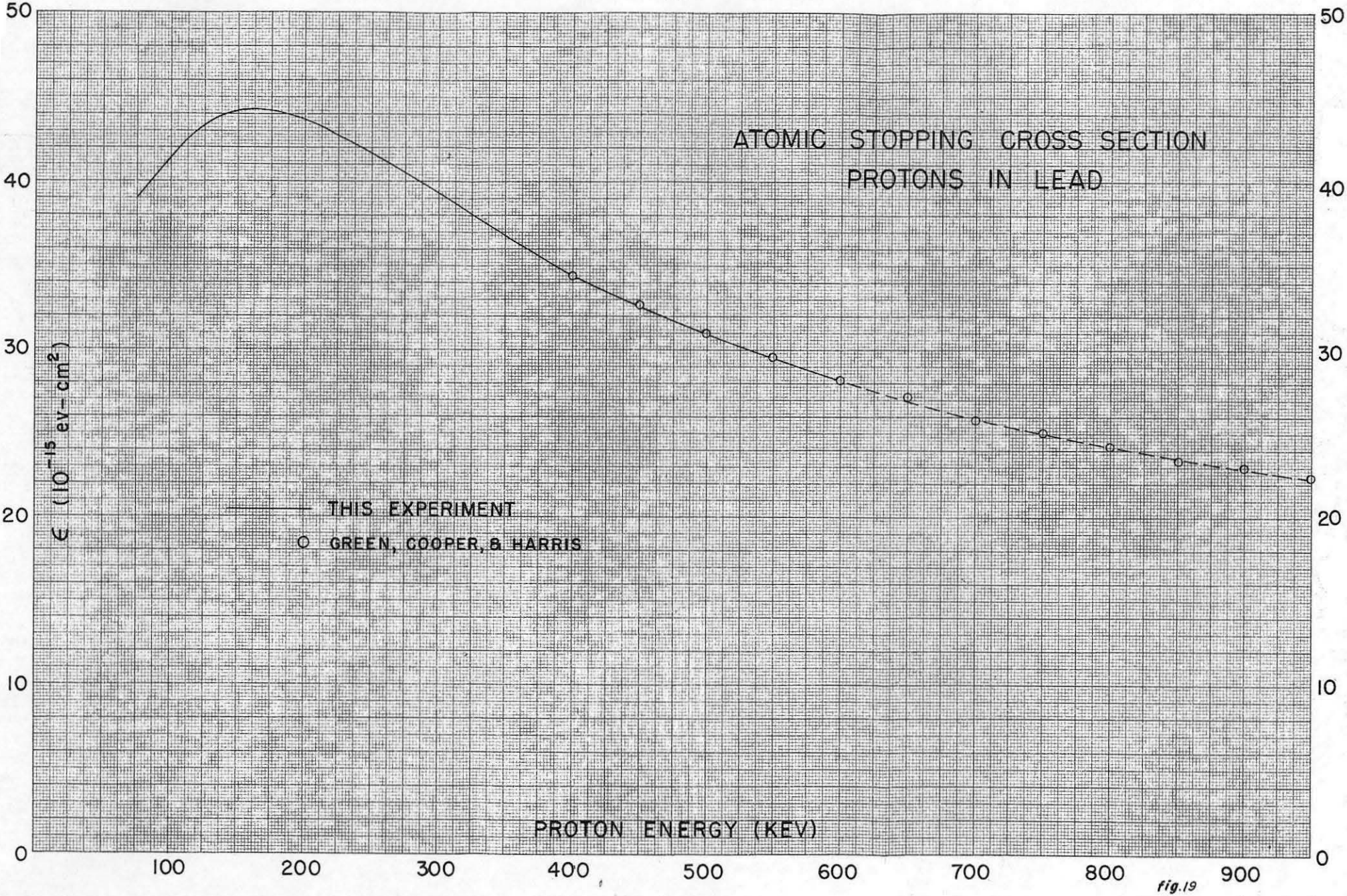
ATOMIC STOPPING CROSS SECTION
PROTONS IN LEAD
ε (10⁻¹⁵ ev-cm²)
THIS EXPERIMENT
GREEN, COOPER, & HARRIS
PROTON ENERGY (KEV)
0
10
20
30
40
50
100
200
300
400
500
600
700
800
900

fig.19

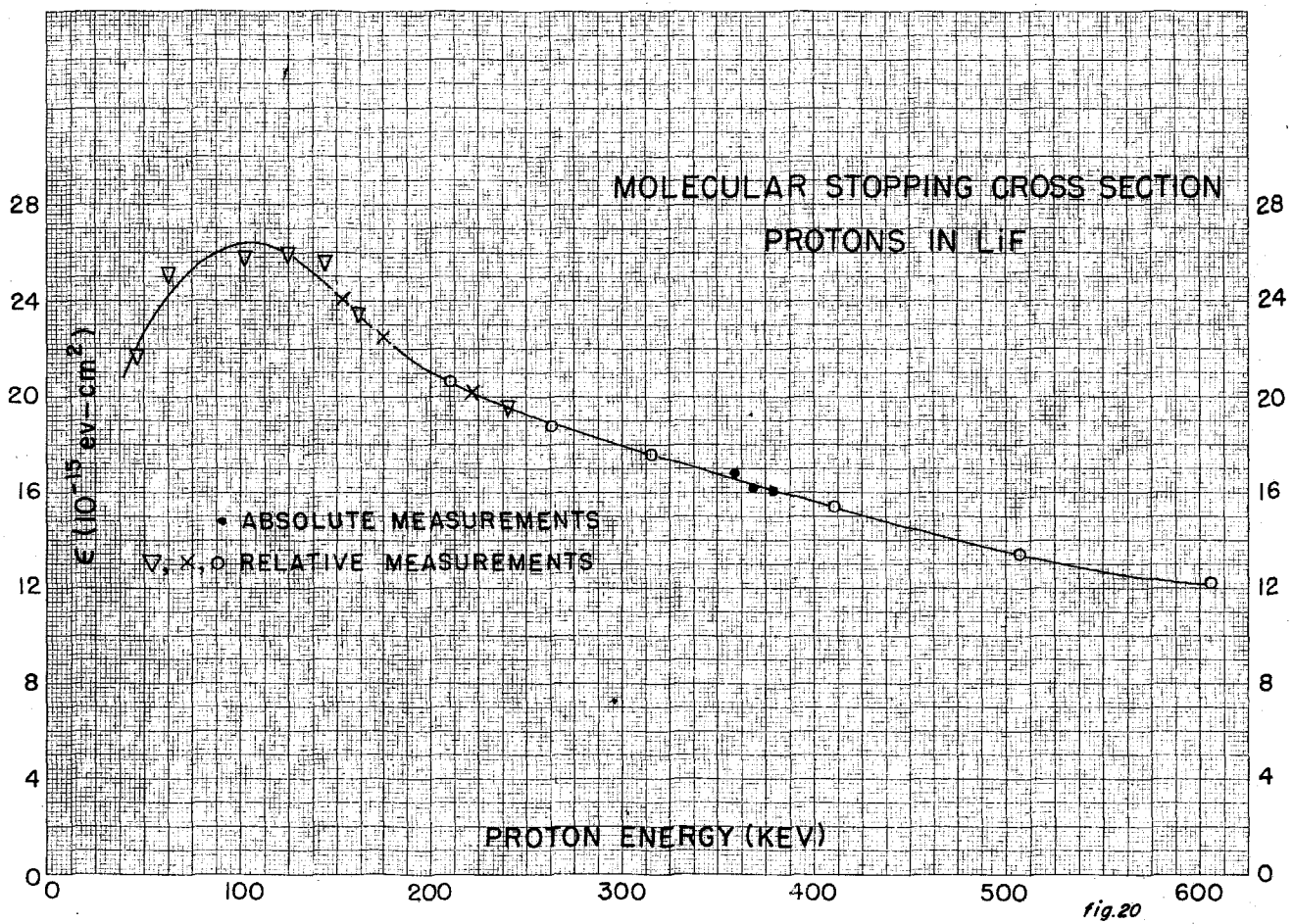
MOLECULAR STOPPING CROSS SECTION
PROTONS IN LiF
ε (10⁻¹⁵ ev-cm²)
• ABSOLUTE MEASUREMENTS
∇, ×, o RELATIVE MEASUREMENTS
PROTON ENERGY (KEV)
0
4
8
12
16
20
24
28
0
100
200
300
400
500
600

fig.20

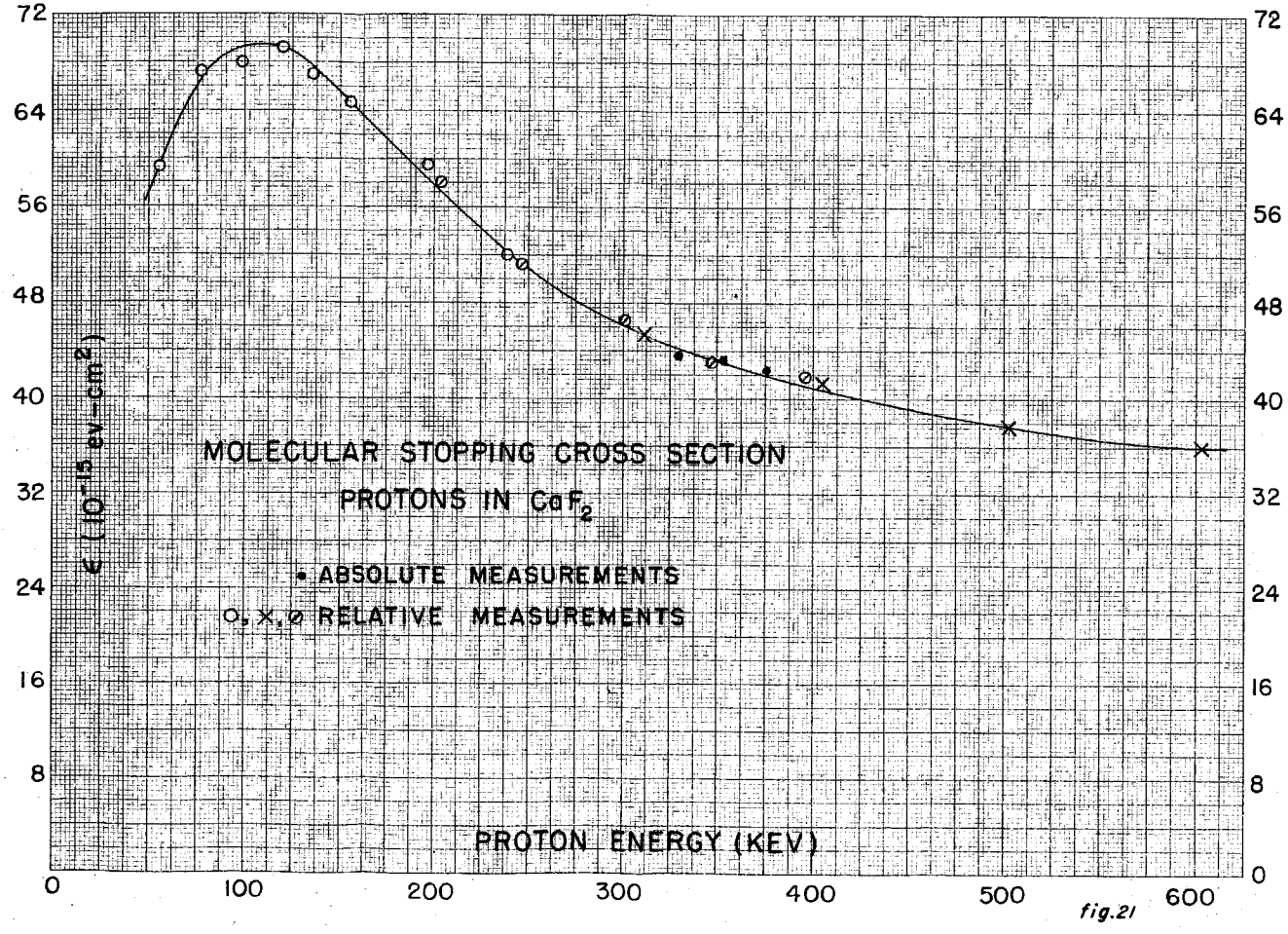
MOLECULAR STOPPING CROSS SECTION
PROTONS IN CaF_2
• ABSOLUTE MEASUREMENTS
O, X, ø RELATIVE MEASUREMENTS
PROTON ENERGY (KEV)
ε (10⁻¹⁵ eV-cm²)
0
100
200
300
400
500
600
8
16
24
32
40
48
56
64
72

fig.21

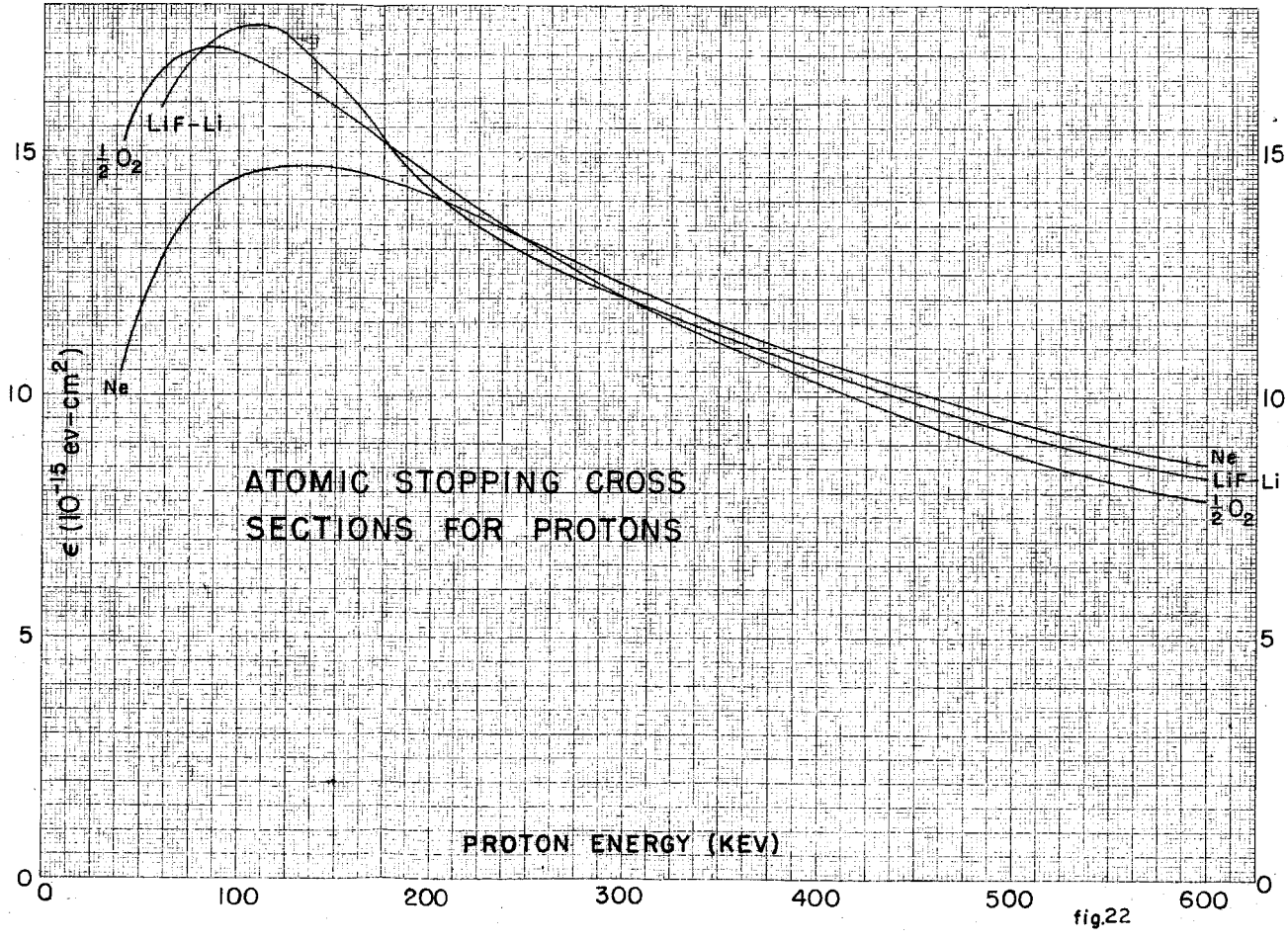
ATOMIC STOPPING CROSS SECTIONS FOR PROTONS
ε (10⁻¹⁵ ev-cm²)
PROTON ENERGY (KEV)
0
5
10
15
100
200
300
400
500
600
LiF-Li
½ O₂
Ne
Ne
LiF-Li
½ O₂

fig.22

REFERENCES

(1) S. Livingston and H. A. Bethe, Revs. Mod. Phys. 9, 264,(1937).

(2) N. Bohr, Kgl. Danske Videnskab Selskab, Mat.-fys. Medd. 18, No. 8 (1948).

(3) S. K. Allison and S. D. Warshaw, Revs. Mod. Phys. 25,779 (1953), and included bibliography.

(4) S. Rosenblum, Ann. de Physique 10, 408 (1928).

(5) L. J. Haworth and L. P. D. King, Phys. Rev. 54, 38, 48 (1938).

(6) W. D. Warters, Ph.D. Thesis, California Institute of Technology (1953).

(7) Warters, Fowler and Lauritsen, Phys. Rev. 91, 917 (1953).

(8) G. Mano, Ann. de Physique 1, 407 (1934)

(9) S. D. Warshaw, Phys. Rev. 76, 1759 (1949).

(10) C. B. Madsen, Dan. Mat. Fys. Medd. 27, No. 13 (1953).

(11) D. Kahn, Phys. Rev. 90, 503 (1953).

(12) C. B. Madsen and P. Venkateswarlu, Phys. Rev. 74, 648, 1783 (1948).

(13) Chilton, Cooper and Harris, Phys. Rev. 93, 413 (1954).

(14) Green, Cooper and Harris, Phys. Rev. (to be published).

(15) T. Huus and C. B. Madsen, Phys. Rev. 76, 323 (1949).

(16) H. A. Wilcox, Phys. Rev. 74, 1743 (1948).

(17) Snyder, Rubin, Fowler and Lauritsen, Rev. Sci. Inst. 21, 852 (1950).

(18) S. D. Warshaw, Rev. Sci. Instr. 20, 623 (1949).

(19) W. A. Wenzel, Ph.D. Thesis, California Institute of Technology (1952).

(20) Caldwell,J.App. Phys. 12, 779 (1941).

(21) Olson and Smith,J.App. Phys. 16, 425 (1945).

(22) F. Mozer, private communication.

(23) R. L. Platzman, "Symposium on Radiobiology," John Wiley & Son, New York, p. 139 (1952).

(24) H. K. Reynolds, Ph.D. Thesis, California Institute of Technology (1953).

(25) Reynolds, Dunbar, Wenzel, and Whaling, Phys. Rev. 92, 742 (1953).

(26) A. H. Morrish, Phys. Rev. 76, 1651 (1949).